SKIN INFLAMMATION

Keratinocyte-intrinsic BCL10/MALT1 activity initiates and amplifies psoriasiform skin inflammation

Zsuzsanna Kurgyis[1,2,3], Larsen Vornholz[1,2], Konstanze Pechloff[1,2], Lajos V. Kemény[4,5], Tim Wartewig[1,2], Andreas Muschaweckh[6], Abhinav Joshi[1,2], Katja Kranen[3], Lara Hartjes[1,2], Sigrid Möckel[3,7], Katja Steiger[8], Erik Hameister[1,2], Thomas Volz[3], Mark Mellett[9], Lars E. French[9,10,11], Tilo Biedermann[3], Thomas Korn[6,12,13], Jürgen Ruland[1,2,14,15]*

Psoriasis is a chronic inflammatory skin disease arising from poorly defined pathological cross-talk between keratinocytes and the immune system. BCL10 (B cell lymphoma/leukemia 10) and MALT1 (mucosa-associated lymphoid tissue lymphoma translocation protein 1) are ubiquitously expressed inflammatory signaling proteins that can interact with the psoriasis susceptibility factor CARD14, but their functions in psoriasis are insufficiently understood. We report that although keratinocyte-intrinsic BCL10/MALT1 deletions completely rescue inflammatory skin pathology triggered by germline *Card14* gain-of-function mutation in mice, the BCL10/MALT1 signalosome is unexpectedly not involved in the CARD14-dependent interleukin-17 receptor (IL-17R) proximal pathway. Instead, it plays a more pleiotropic role by amplifying keratinocyte responses to a series of inflammatory cytokines, including IL-17A, IL-1β, and TNF. Moreover, selective keratinocyte-intrinsic activation of BCL10/MALT1 signaling with an artificial engager molecule is sufficient to initiate lymphocyte-mediated psoriasiform skin inflammation, and aberrant BCL10/MALT1 activity is frequently detected in the skin of human sporadic psoriasis. Together, these results establish that BCL10/MALT1 signalosomes can act as initiators and crucial amplifiers of psoriatic skin inflammation and indicate a critical function for this complex in sporadic psoriasis.

INTRODUCTION

Psoriasis is a chronic inflammatory skin disease that affects 2 to 3% of the general population (*1*). Debilitating skin lesions and associated systemic comorbidities severely impair patient quality of life (*2*). Histopathologically, the scaling and itching skin of patients with psoriasis is characterized by hyperproliferative keratinocytes and mixed inflammatory infiltrates that mainly consist of lymphocytes and neutrophil granulocytes. Although the pathological interplay between keratinocytes and the innate and adaptive immune systems is known to drive pathogenesis, the underlying mechanisms have been insufficiently defined.

In most cases, psoriasis is based on a complex genetic trait; therefore, several genome-wide association studies (GWAS) have been performed (*3*–*6*). These studies have revealed that a large number of psoriasis susceptibility genes are linked to the inflammatory nuclear factor κB (NF-κB) pathway (e.g., *CARD14*, *NFKBIA*, *NFKBIZ*, *REL*, *TNFAIP3*, and *TNIP1*) or directly to the interleukin-23 (IL-23)/T helper 17 (T_H17) signaling axis (e.g., *IL12B*, *IL23A*, *IL23R*, *JAK2*, *STAT3*, *TRAF3IP2*, and *TYK2*). Individually, most of these risk factors confer only a low risk of disease development (odds ratio < 1.5). However, caspase recruitment domain family member 14 (*CARD14*) has not only been linked to psoriasis susceptibility locus 2 (PSORS2) by GWAS but has also been causally connected to rare forms of familial psoriasis (*7*–*10*) and the related inflammatory skin disease pityriasis rubra pilaris (*11*–*13*), indicating that it controls particularly important pathways for these disorders.

CARD14 (or CARMA2) is a proinflammatory signaling molecule that is physiologically expressed in several cell types in the skin, including keratinocytes (*7*), Langerhans cells (*14*), dermal γδ T cells (*14*), and endothelial cells (*15*); in the placenta (*16*); and gut (*11*). This molecule contains an N-terminal CARD, a central coiled-coil (CC) and linker domain, and a C-terminal membrane-associated guanylate kinase (MAGUK) region (*17*). Psoriasis-associated gain-of-function (GOF) mutations result in structural alterations within CARD14 that disrupt intramolecular autoinhibition and lead to constitutive activation of the NF-κB pathway in vitro and in vivo (*18*, *19*). Recently developed knock-in mouse models that have psoriasis-associated *Card14* mutations in their germline or in keratinocytes develop psoriasiform skin inflammation with histopathological features of human psoriasis, demonstrating that these alterations are sufficient to drive pathology (*19*–*22*). In this context, it has been demonstrated that CARD14 acts proximally at the IL-17 receptor (IL-17R) and links IL-17R ligation to activation of the canonical inhibitor of nuclear factor κB (IκB) kinase (IKK)–induced NF-κB signaling pathway via a direct interaction with the ubiquitin ligase tumor necrosis factor receptor–associated factor 6 (TRAF6) and the adapter protein ACT1 (*21*), which has been suggested to explain the pathogenic role of *CARD14-GOF* alterations in inherited skin inflammation (*21*, *23*).

[1]Institute of Clinical Chemistry and Pathobiochemistry, School of Medicine, Technical University of Munich, Munich, Germany. [2]TranslaTUM, Center for Translational Cancer Research, Technical University of Munich, Munich, Germany. [3]Department of Dermatology and Allergy, Technical University of Munich, Munich, Germany. [4]Cutaneous Biology Research Center, Department of Dermatology and MGH Cancer Center, Massachusetts General Hospital, Harvard Medical School, Boston, MA, USA. [5]Department of Dermatology, Venereology, and Dermatooncology, Faculty of Medicine, Semmelweis University, Budapest, Hungary. [6]Department of Experimental Neuroimmunology, Klinikum rechts der Isar, Technical University of Munich, Munich, Germany. [7]Institute of Pathology, Universität Würzburg, Würzburg, Germany. [8]Institute of Pathology, School of Medicine, Technical University of Munich, Munich, Germany. [9]Department of Dermatology, University Hospital of Zürich, University of Zurich (UZH), Zürich, Switzerland. [10]Department of Dermatology and Allergy, University Hospital, LMU Munich Munich, Germany. [11]Dr. Phillip Frost Department of Dermatology and Cutaneous Surgery, University of Miami Miller School of Medicine, Miami, FL, USA. [12]Department of Neurology, Klinikum rechts der Isar, Technical University of Munich, Munich Germany. [13]Munich Cluster for Systems Neurology (SyNergy), Munich, Germany. [14]German Cancer Consortium (DKTK), Heidelberg, Germany. [15]German Center for Infection Research (DZIF), Munich partner site, Munich Germany.
*Corresponding author. Email: j.ruland@tum.de

In addition to interacting with TRAF6 and ACT1, CARD14 also binds via its CARD domain to the CARD of the adaptor molecule BCL10 (B cell lymphoma/leukemia 10) (*16*–*18*, *24*–*26*), which constitutively interacts with the paracaspase MALT1 (mucosa-associated lymphoid tissue lymphoma translocation 1) (*17*). BCL10 and MALT1 form ubiquitously expressed signalosomes, which can be activated by a large series of upstream stimuli in different cell types (*17*), including antigen receptor signals in lymphocytes; microbial signals via pattern recognition receptors such as Dectin-1 or via receptor tyrosine kinases; and G protein–coupled receptors in innate immune cells and in nonhematopoietic tissues, including the skin (*17*). Activation of the BCL10/MALT1 signaling module triggers IKK-mediated NF-κB signaling as well as the p38 and c-Jun N-terminal kinase (JNK) cascades (*17*). In addition, MALT1 functions as a cysteine protease that can cleave an array of inflammatory regulators to provide an additional layer of context-specific gene expression control (*17*). Although psoriasis-associated CARD14-GOF variants can constitutively assemble and activate the BCL10/MALT1 module (*18*, *19*), the molecular and cellular functions of this signalosome in the complex pathogenesis of psoriasis are insufficiently defined.

To explore the roles of BCL10 and MALT1 in inflammatory skin disease, we engineered a series of conditional mouse mutants to specifically activate, inactivate, or attenuate BCL10/MALT1 signaling in keratinocytes in vivo. We report that although keratinocyte-intrinsic BCL10/MALT1 complexes are absolutely critical for skin inflammation triggered by germline *Card14-GOF* mutations, the BCL10/MALT1 complex is unexpectedly not involved in IL-17R proximal events. Instead, it amplifies keratinocyte responses to multiple proinflammatory cytokines. In addition, keratinocyte-intrinsic activation of BCL10/MALT1 signaling alone is sufficient to drive psoriasiform skin inflammation in vivo, and altered BCL10/MALT1 signaling is frequently detected in human sporadic psoriasis.

RESULTS

Keratinocyte-intrinsic BCL10/MALT1 signaling mediates *Card14Δ^{E138}* and chemically induced skin inflammation

Knock-in mice with a psoriasis-associated germline mutation in the *Card14* locus spontaneously develop chronic skin inflammation with features of human psoriasis (*19*–*21*). Because CARD14 is expressed in several cell types (*7*, *11*, *14*, *15*), we first explored the keratinocyte-intrinsic functions of BCL10 and MALT1 in *Card14^{ΔE138}* mice by crossing these animals to mice that harbor homozygous conditional *Bcl10* (*27*) or *Malt1* (*27*) alleles and a keratinocyte-specific *Cre* driven by the *Keratin14* promoter (*Bcl10^{KC-KO}* and *Malt1^{KC-KO}*) (*28*). Compound mutant mice harbor a *Card14^{ΔE138}* GOF allele in all cell types and keratinocyte-specific deletions of either the *Bcl10* (*Card14^{ΔE138};Bcl10^{KC-KO}*) (Fig. 1A) or *Malt1* locus (*Card14^{ΔE138};Malt1^{KC-KO}*). Keratinocyte-specific deletion of either *Bcl10* or *Malt1* completely rescued the chronic skin inflammation driven by *Card14^{ΔE138}*, as *Card14^{ΔE138};Bcl10^{KC-KO}* and *Card14^{ΔE138};Malt1^{KC-KO}* mice displayed no macroscopic signs of inflammation (fig. S1, A and B), and the characteristic ear thickening of *Card14^{ΔE138}* animals was also absent (Fig. 1, B and C). The histological analysis of *Card14^{ΔE138}* mice showed in the presence of BCL10 and MALT1 an acanthotic epidermis with focal hypogranulosis and mounds of parakeratosis housing neutrophils, dilated capillaries, and a perivascular infiltrate with lymphocytes and neutrophils characteristic of psoriasiform skin inflammation. All these pathological features were completely absent in the skin of *Card14^{ΔE138};Bcl10^{KC-KO}* and *Card14^{ΔE138};Malt1^{KC-KO}* animals (Fig. 1, D and E).

Flow cytometric analysis confirmed the increased numbers of skin-infiltrating neutrophil granulocytes and αβ T cells, including those expressing IL-17A, in *Card14^{ΔE138}* mice, whereas γδ T cell counts were normal. These pathological infiltrates were also not detected upon keratinocyte-intrinsic *Bcl10* or *Malt1* deletion (Fig. 1, F to K, and fig. S1, C to F). In addition, the IL-17 target genes *Cxcl1*, *Csf2*, *S100a8*, *Lcn2*, and *Tnf* were elevated in the skin of *Card14^{ΔE138}* mice but not in the skin of *Card14^{ΔE138};Bcl10^{KC-KO}* and *Card14^{ΔE138};Malt1^{KC-KO}* animals (fig. S1, G to P). Together, these results establish, at the genetic level, that keratinocyte-intrinsic activation of BCL10/MALT1 signaling is absolutely critical for psoriasiform skin inflammation triggered by a germline *Card14-GOF* mutation.

To study the role of keratinocyte-intrinsic BCL10/MALT1 signalosomes in an alternative and well-established murine model of psoriasis, we next used *Bcl10^{KC-KO}* mice and treated them with the imiquimod-containing cream Aldara (*29*). Imiquimod is a Toll-like receptor 7/9 (TLR7/9) agonist that induces IL-17A–dependent psoriasis-like skin inflammation (*29*). The daily topical application of imiquimod to the back and ears of wild-type mice led, as expected, to strong skin inflammation with local swelling (Fig. 1, L and M), the infiltration of neutrophils as well as αβ T cells and IL-17A–expressing αβ T cells (Fig. 1, N to P), and the expression of various cytokines and chemokines, such as *Cxcl1*, *Lcn2*, *S100a8*, and *S100a9* (Fig. 1, Q to T), as previously described (*29*). In the absence of keratinocyte-intrinsic BCL10, this inflammatory response was significantly reduced but did not abate the signal completely (Fig. 1, L to T).

BCL10/MALT1 activation in keratinocytes drives psoriasiform skin inflammation

After establishing a keratinocyte-intrinsic requirement of BCL10/MALT1 signaling complexes in genetic and chemically induced skin inflammation, we next were interested in whether selectively enforced activation of BCL10/MALT1 signaling only within keratinocytes would be sufficient to trigger pathology. To explore this question in the absence of CARD14-GOF, which could have additional effects, such as in the IL-17R proximal pathway (*21*), we engineered an experimental BCL10/MALT1 engager molecule based on the protein CARD11, which is normally mostly expressed in lymphocytes in addition to mast cells and in the skin (*17*, *30*, *31*). To create a constitutively active form of CARD11, we deleted the autoinhibitory CARD-MAGUK linker domain (*32*) and termed this BCL10/MALT1 activator CARD11^{ΔLinker}. To engage BCL10/MALT1 signalosomes in a cell-type specific manner in vivo, we next introduced *Card11^{ΔLinker}* cDNA together with green fluorescent protein (GFP) cDNA, preceded by a loxP-flanked STOP cassette, in the ubiquitously expressed *Rosa26* locus (fig. S2, A and B). For keratinocyte-specific expression, we crossed these animals with *K14Cre* mice (Fig. 2A for schematic). In the offspring (*Card11$^{ΔLinker-KC}$* mice), we detected keratinocyte-intrinsic expression of CARD11^{ΔLinker} (fig. S2C).

All *Card11$^{ΔLinker-KC}$* mice developed an inflammatory skin disorder characterized by scaling, thickening, and redness of the ears with 100% penetrance (Fig. 2B). Keratinocytes isolated from *Card11$^{ΔLinker-KC}$* mice exhibited increased NF-κB activity (Fig. 2C) and cell-autonomous inflammatory gene expression without exogenous stimulation (Fig. 2D). Crosses of *Card11$^{ΔLinker-KC}$* mice to *Bcl10^{KC-KO}* or *Malt1^{KC-KO}* mice completely rescued the phenotype (Fig. 2E), demonstrating that the keratinocyte-intrinsic activation of BCL10/MALT1 signaling was

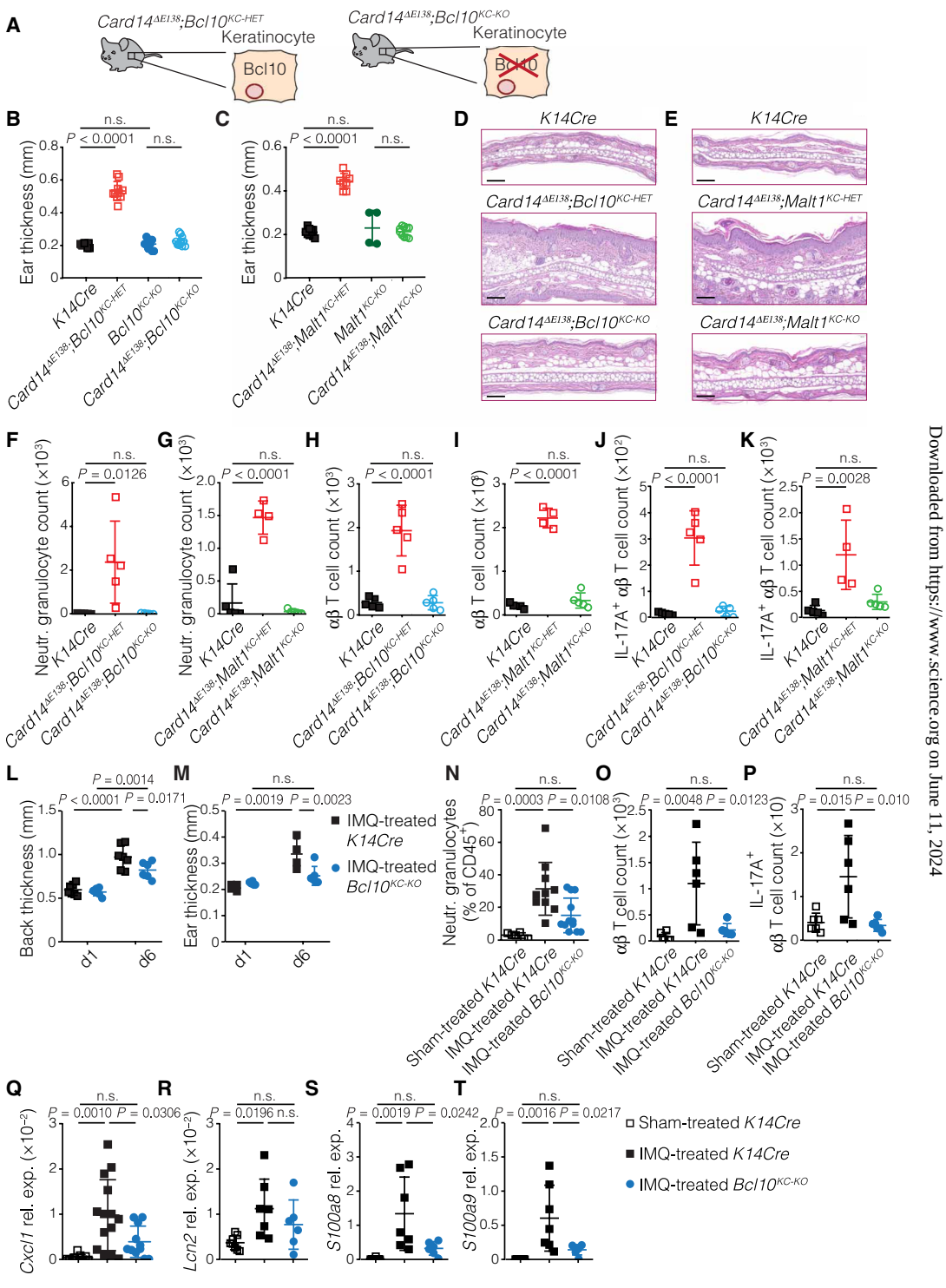

Fig. 1. Keratinocyte-intrinsic BCL10/MALT1 signaling mediates mutant CARD14-triggered and chemically induced skin inflammation. (**A**) Schematics of mice with activating germline mutation in the murine *Card14* gene without (*Card14*$^{\Delta E138}$;*Bcl10*$^{KC\text{-}HET}$) or with keratinocyte-intrinsic deletion of *Bcl10* (*Card14*$^{\Delta E138}$;*Bcl10*$^{KC\text{-}KO}$). (**B** and **C**) Ear thickness of *K14Cre* (B) *Card14*$^{\Delta E138}$;*Bcl10*$^{KC\text{-}HET}$, *Card14*$^{\Delta E138}$;*Bcl10*$^{KC\text{-}KO}$, and *Bcl10*$^{KC\text{-}KO}$ and (C) *Card14*$^{\Delta E138}$;*Malt1*$^{KC\text{-}HET}$, *Card14*$^{\Delta E138}$;*Malt1*$^{KC\text{-}KO}$, and *Malt1*$^{KC\text{-}KO}$ mice. n.s., not significant. (**D** and **E**) Representative histological sections showing acanthotic epidermis with focal hypogranulosis and mounds of parakeratosis housing neutrophils, a few mitoses in the basal epidermis, dilated capillaries and perivascular infiltrates with lymphocytes and neutrophils in the ears of (D, middle) *Card14*$^{\Delta E138}$;*Bcl10*$^{KC\text{-}HET}$ and (E, middle) *Card14*$^{\Delta E138}$;*Malt1*$^{KC\text{-}HET}$ mice. No skin alterations were observed in (D, bottom) *Card14*$^{\Delta E138}$;*Bcl10*$^{KC\text{-}KO}$ and (E, bottom) *Card14*$^{\Delta E138}$;*Malt1*$^{KC\text{-}KO}$ mice and (D and E, top) *K14Cre* littermate controls. (**F** and **G**) Quantification by flow cytometry of Ly6G$^+$ CD11b$^+$ neutrophil granulocytes from the ears of *K14Cre* (F) *Card14*$^{\Delta E138}$;*Bcl10*$^{KC\text{-}HET}$ and *Card14*$^{\Delta E138}$;*Bcl10*$^{KC\text{-}KO}$ and (G) *Card14*$^{\Delta E138}$;*Malt1*$^{KC\text{-}HET}$ and *Card14*$^{\Delta E138}$;*Malt1*$^{KC\text{-}KO}$ mice. (**H** and **I**) Quantification by flow cytometry of TCRγ–TCRβ$^+$ αβ T cells from the ears of *K14Cre* (H) *Card14*$^{\Delta E138}$;*Bcl10*$^{KC\text{-}HET}$ and *Card14*$^{\Delta E138}$;*Bcl10*$^{KC\text{-}KO}$ and (I) *Card14*$^{\Delta E138}$;*Malt1*$^{KC\text{-}HET}$ and *Card14*$^{\Delta E138}$;*Malt1*$^{KC\text{-}KO}$ mice. (**J** and **K**) Quantification by flow cytometry of IL-17A$^+$ TCRγ–TCRβ$^+$ αβ T cells from the ears of *K14Cre* (J) *Card14*$^{\Delta E138}$;*Bcl10*$^{KC\text{-}HET}$ and *Card14*$^{\Delta E138}$;*Bcl10*$^{KC\text{-}KO}$ and (K) *Card14*$^{\Delta E138}$;*Malt1*$^{KC\text{-}HET}$ and *Card14*$^{\Delta E138}$;*Malt1*$^{KC\text{-}KO}$ mice. (**L** and **M**) Back and ear skin thickness of *K14Cre* and *Bcl10*$^{KC\text{-}KO}$ mice before and after 5 days of imiquimod treatment. (**N**) Quantification by flow cytometry of Ly6G$^+$ CD11b$^+$ neutrophil granulocytes from the backs and ears of *K14Cre* and *Bcl10*$^{KC\text{-}KO}$ mice after 5 days of imiquimod or sham treatment. (**O** and **P**) Quantification by flow cytometry of (O) TCRγ–TCRβ$^+$ αβ T cells and (P) IL-17A$^+$ TCRγ–TCRβ$^+$ αβ T cells from the ears of *K14Cre* and *Bcl10*$^{KC\text{-}KO}$ mice after 5 days of imiquimod or sham treatment. (**Q**) Relative mRNA expression in the back and ears of *K14Cre* and *Bcl10*$^{KC\text{-}KO}$ mice after 5 days of imiquimod or sham treatment. (**R** to **T**) Relative mRNA expression in the ears of *K14Cre* and *Bcl10*$^{KC\text{-}KO}$ mice after 5 days of imiquimod or sham treatment. Each data point represents (B, C, F to M, O, P, and R to T) a single mouse or (N and Q) a treated organ (back or ear) of a mouse. Means ± SD. Data are (F to K) representative of or (L to T) pooled from $n = 2$ independent experiments. (B, C, F to K, and N to T) Ordinary one-way analysis of variance (ANOVA) with Tukey's post hoc test or (L and M) two-way ANOVA with Sidak's post hoc test. Scale bars, 200 μm.

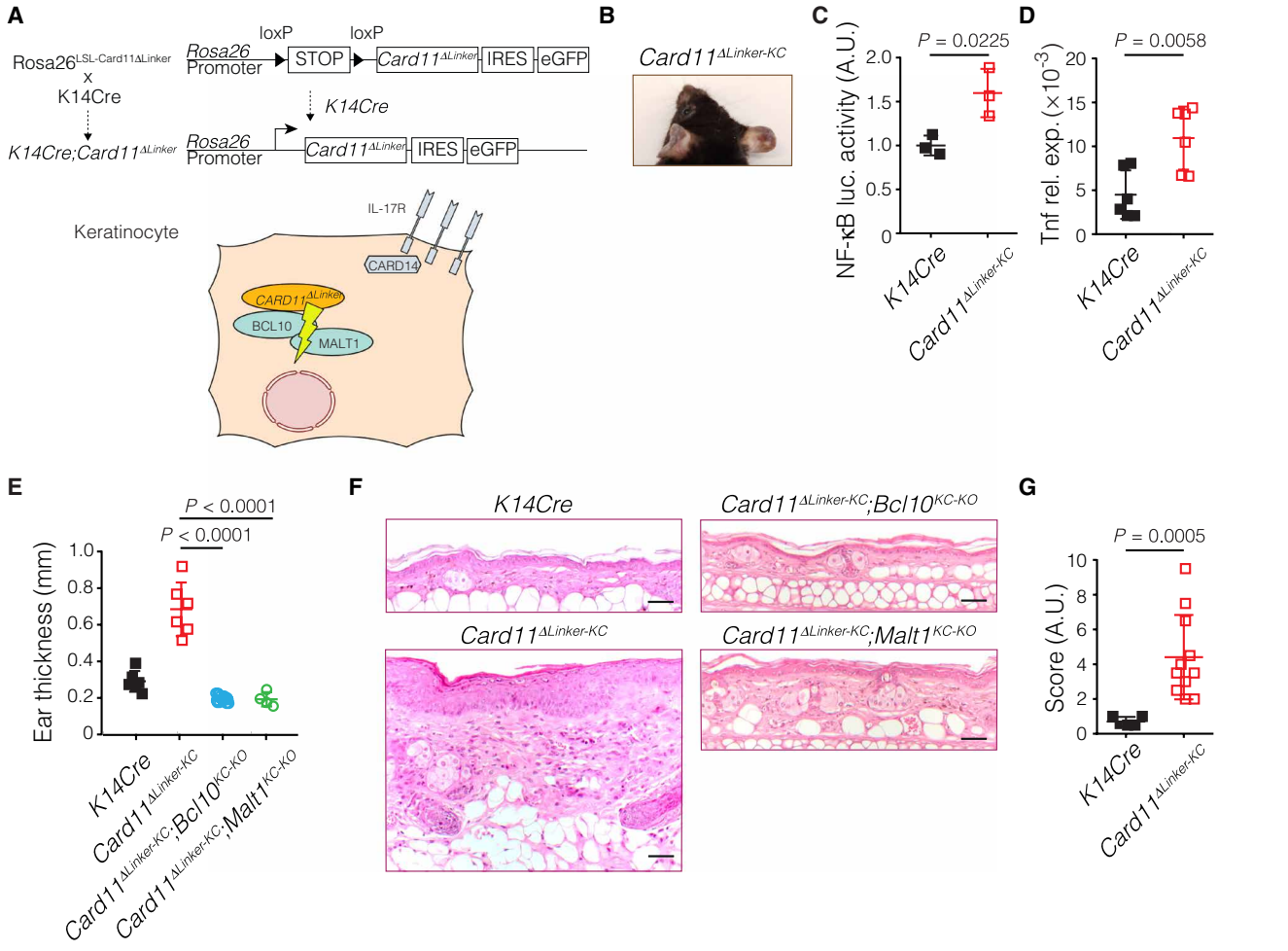

Fig. 2. BCL10/MALT1 activation in keratinocytes drives psoriasiform skin inflammation. (**A**) Schematics of mice with conditional expression of *Card11*$^{\Delta Linker}$ cDNA from the *Rosa26* locus. In keratinocytes, where the K14 promoter drives Cre expression, Cre-mediated excision of the STOP cassette results in *Card11*$^{\Delta Linker}$ expression and thereby activation of keratinocyte BCL10/MALT1 complexes. (**B**) Representative image of the ears of *Card11*$^{\Delta Linker\text{-}KC}$ mice. (**C**) NF-κB luciferase reporter assay in keratinocytes isolated from *Card11*$^{\Delta Linker\text{-}KC}$ mice and *K14Cre* littermate controls that were cultured and transfected with NF-κB and control luciferase reporter plasmids. A.U., arbitrary units. (**D**) Relative mRNA expression in keratinocytes isolated from *Card11*$^{\Delta Linker\text{-}KC}$ mice and *K14Cre* littermate controls. (**E**) Ear thickness of *Card11*$^{\Delta Linker\text{-}KC}$, *Card11*$^{\Delta Linker\text{-}KC}$*;Bcl10*$^{KC\text{-}KO}$ and *Card11*$^{\Delta Linker\text{-}KC}$*;Malt1*$^{KC\text{-}KO}$ mice and *K14Cre* littermate controls. (**F**) Representative histological sections (left, bottom) showing acanthotic epidermis with hypogranulosis and slight hypokeratosis, basal mitoses in the epidermis, and perivascular infiltrate with lymphocytes and neutrophils in the ears of *Card11*$^{\Delta Linker\text{-}KC}$ mice. (Left, top) No skin lesions were observed in *K14Cre* littermates. Representative histological sections from the ears of (right, top) *Card11*$^{\Delta Linker\text{-}KC}$*;Bcl10*$^{KC\text{-}KO}$ and (right, bottom) *Card11*$^{\Delta Linker\text{-}KC}$*;Malt1*$^{KC\text{-}KO}$ mice showing the absence of epidermal thickening and inflammatory infiltrates. (**G**) Baker's psoriasis histology scores based on the examination of the ears of *Card11*$^{\Delta Linker\text{-}KC}$ mice and *K14Cre* littermate controls. Each data point represents a single mouse (C to E and G). Means ± SD. Data are representative of $n = 2$ (C and D) independent experiments. (E) Ordinary one-way ANOVA with Tukey's post hoc test or (C and D) Student's *t* test. Scale bars, 200 μm.

responsible for driving this disease. Histopathological analysis of *Card11*$^{\Delta Linker\text{-}KC}$ mice demonstrated acanthosis, lymphocytic and neutrophil granulocytic infiltration, and increased vascularization, which are classical characteristics of psoriasis (Fig. 2, F and G). Quantification of the histological signs observed in *K14Cre;Card11*$^{\Delta Linker}$ mice using the psoriasis histology score developed by Baker *et al.* (*33*) confirmed the resemblance to psoriatic lesions (Fig. 2F), which were completely absent in animals lacking either keratinocyte BCL10 or MALT1 (Fig. 2G).

Similar to patients with psoriasis, *Card11*$^{\Delta Linker\text{-}KC}$ animals showed increased numbers of neutrophil granulocytes in the skin (Fig. 3A and fig. S3A) and αβ T cells (Fig. 3B and fig. S3B), whereas dermal γδ T cell counts were comparable with those in control littermates (fig. S3, B and C). In particular, IL-17A–producing αβ T cells were expanded (Fig. 3C), whereas the numbers of IL-17A$^+$ γδ T cells were not increased (fig. S3D). Moreover, mRNA expression analyses of the inflamed skin tissue revealed the up-regulation of *Il17a* transcripts (Fig. 3D), whereas the expression of the T_H1 and T_H2 signature cytokines *Ifng* and *Il4* was not increased in *Card11*$^{\Delta Linker\text{-}KC}$ animals (Fig. 3, E and F). We also found increased expression of *Ccl20* (Fig. 3G), a major chemokine attracting CCR6$^+$ and IL-17A–expressing T cells (*34*), which might explain their high numbers in the skin. In line with enhanced IL-17A–mediated pathology, the IL-17 target genes *Cxcl1* and *Cxcl5* as well as *Csf2* were also up-regulated in the inflamed skins of *Card11*$^{\Delta Linker\text{-}KC}$ mice (Fig. 3H), which likely explains the high numbers of infiltrating granulocytes. Additional IL-17 target genes,

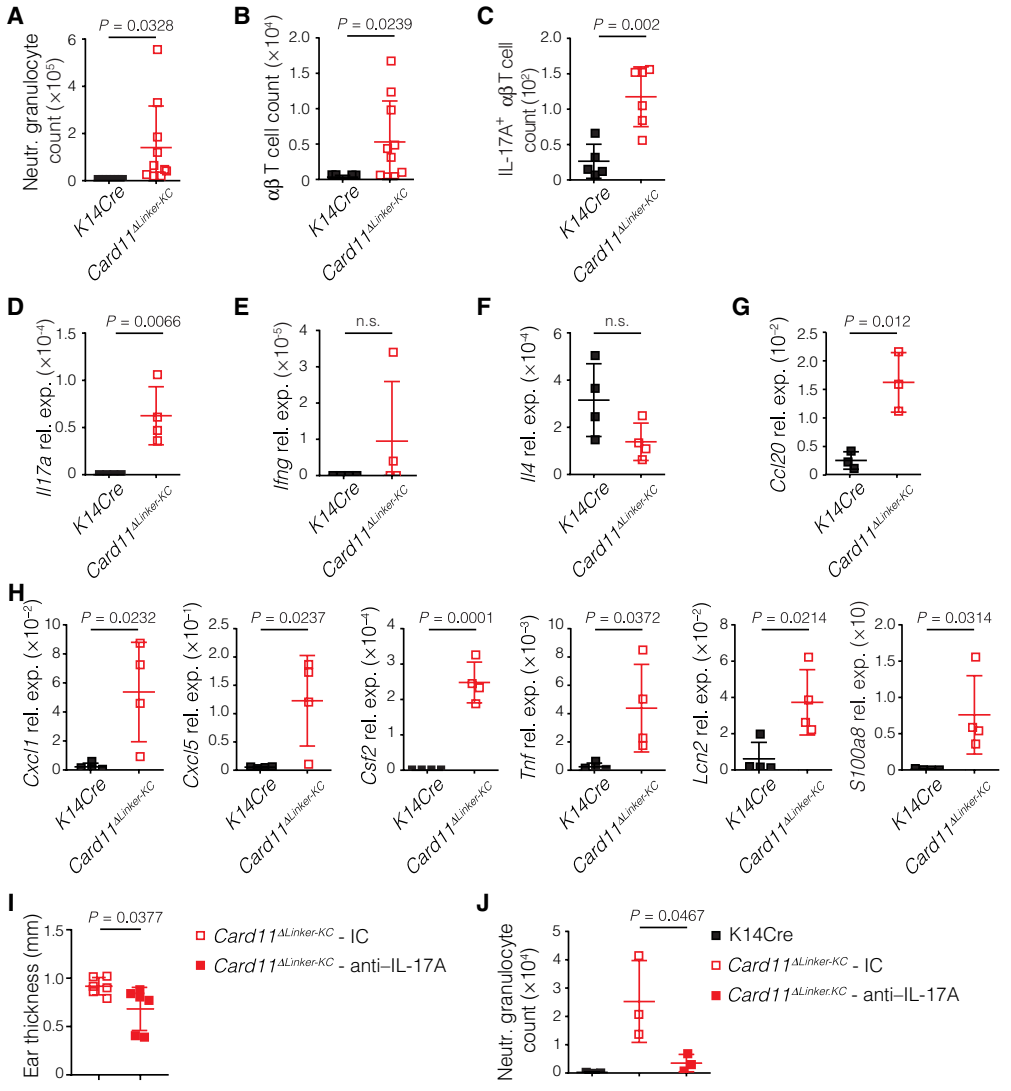

Fig. 3. Skin inflammation mediated by keratinocyte BCL10/MALT1 shows the characteristics of human psoriasis. (**A**) Quantification by flow cytometry of Ly6G$^+$ CD11b$^+$ neutrophil granulocytes from the ears of *Card11*$^{\Delta Linker\text{-}KC}$ mice and *K14Cre* littermate controls. (**B**) Quantification by flow cytometry of TCRγ–TCRβ$^+$ αβ T cells from the ears of *Card11*$^{\Delta Linker\text{-}KC}$ mice and *K14Cre* littermate controls. (**C**) Quantification by flow cytometry of IL-17A$^+$ TCRγ–TCRβ$^+$ αβ T cells from the ears of *Card11*$^{\Delta Linker\text{-}KC}$ mice and *K14Cre* littermate controls. (**D** to **H**) Relative mRNA expression in the ears of *Card11*$^{\Delta Linker\text{-}KC}$ mice and *K14Cre* littermate controls. (**I**) Ear thickness of *Card11*$^{\Delta Linker\text{-}KC}$ mice and (**J**) quantification of Ly6G$^+$ CD11b$^+$ neutrophil granulocytes from the ears of *Card11*$^{\Delta Linker\text{-}KC}$ mice treated with 200 μg of anti–IL-17A or isotype control (IC) intraperitoneally for 14 days and *K14Cre* littermate controls. Each data point represents a single mouse. Means ± SD. Data are (A to C) pooled from $n = 2$ independent experiments or are (D and J) representative of $n = 2$ independent experiments. (A to I) Student's *t* test or (J) ordinary one-way ANOVA with Tukey's post hoc test.

such as *S100a8*, *Lcn2*, and *Tnf*, were also up-regulated in *Card11*$^{\Delta Linker\text{-}KC}$ skins (Fig. 3H). Again, the expression of IL-17 target genes was not enhanced in *Card11*$^{\Delta Linker\text{-}KC}$;*Bcl10*$^{KC\text{-}KO}$ and *Card11*$^{\Delta Linker\text{-}KC}$;*Malt1*$^{KC\text{-}KO}$ mice (fig. S3, E and F). Furthermore, treatment of *Card11*$^{\Delta Linker\text{-}KC}$ animals with anti–IL-17A significantly decreased the skin thickness (Fig. 3I) and reduced neutrophil granulocyte numbers to wild-type levels (Fig. 3J). Thus, keratinocyte-intrinsic activation of the BCL10/MALT1 signalosome by CARD11$^{\Delta Linker}$ drives T_H17-dominated psoriasiform skin inflammation with key characteristics of human psoriasis.

Enforced BCL10/MALT1 signaling in keratinocytes triggers lymphocyte-mediated pathology

To understand the mechanisms of keratinocyte-intrinsic CARD11$^{\Delta Linker}$/BCL10/MALT1-induced skin inflammation and to specifically explore the role of lymphocytes in this pathology, we next crossed *Card11*$^{\Delta Linker\text{-}KC}$ mice with *Rag2*-deficient animals that lack T and B cells (*35*). Although *Card11*$^{\Delta Linker\text{-}KC}$;*Rag2*$^{-/-}$ mice showed increased epidermal thickening and keratinization (Fig. 4A) with an up-regulation of the keratinocyte activation and proliferation markers *Krt6* and *Krt16* (Fig. 4B) (*36*, *37*), expression of the T_H17 target genes *Cxcl1*, *Cxcl5*, *Csf2*, *Lcn2*, and *Tnf* was, in contrast to *Card11*$^{\Delta Linker\text{-}KC}$ mice, not increased in *Card11*$^{\Delta Linker\text{-}KC}$;*Rag2*$^{-/-}$ animals (Fig. 4C). Moreover, although some ear swelling was detectable, most likely because of epidermal changes, their ear thickness was greatly reduced in comparison with that of *Card11*$^{\Delta Linker\text{-}KC}$ mice (Fig. 4D), and the strong neutrophilic infiltration seen in the skin of *Card11*$^{\Delta Linker\text{-}KC}$ mice was not observed in *Card11*$^{\Delta Linker\text{-}KC}$;*Rag2*$^{-/-}$ animals (Fig. 4E). Thus, although keratinocyte-intrinsic CARD11$^{\Delta Linker}$ signaling can drive keratinocyte activation and hyperkeratosis, the presence of lymphocytes is necessary to induce full psoriasiform pathology.

BCL10/MALT1 signaling in keratinocytes amplifies secondary cytokine circuits

In psoriasis, lymphocyte-derived cytokines can stimulate keratinocytes, which then amplify inflammation (*38*). To test the keratinocyte-intrinsic roles of BCL10 and MALT1 in secondary cytokine-induced keratinocyte responses, we isolated keratinocytes from *Bcl10*$^{-/-}$ (*39*) or *Malt1*$^{-/-}$ mice (*40*) and stimulated them with psoriasis-related and lymphocyte-derived factors IL-17A, IL-1β, or tumor necrosis factor (TNF) (Fig. 5A for schematic). In the absence of BCL10, IL-17A, IL-1β, and TNF were unable to induce the regular expression of their target genes *Tnf*, *Cxcl5*, and *Csf2* (Fig. 5, B to E). Likewise, *Malt1*-deficient keratinocytes (*40*) were also substantially impaired in inducing *Tnf*, *Cxcl5*, and *Csf2* expressions upon IL-17A or IL-1β stimulation

(Fig. 5, F to I). In contrast, *Card11*$^{\Delta Linker\text{-}KC}$ keratinocytes with activated BCL10/MALT1 signaling exhibited substantial increases in the levels of *Tnf*, *Cxcl5*, and *Csf2* production in response to IL-17A or IL-1β stimulation (fig. S4, A to C). Thus, although the enforced activation of the BCL10/MALT1 signalosome in keratinocytes can amplify inflammatory responses to several cytokines, the presence of endogenous BCL10 and MALT1 is essential for the normal keratinocyte response to IL-17A and IL-1β or TNF. This effect is not due to altered cytokine receptor expression because *Bcl10*-deficient keratinocytes had normal *Il17ra*, *Tnfrsf1*, and *Il1r* expression (fig. S4, D to F) and the surface expression of the IL-17R was also unaltered (fig. S4G). Furthermore, *Bcl10*- or *Malt1*-deficient keratinocytes were not completely unresponsive to exogenous stimuli, as the IL-17A–, IL-1β–, and TNF-induced expression of *Nfkbiz* (encoding IκBζ), which is a gene also linked to psoriasis pathogenesis (*41*, *42*), was unaffected in the absence of BCL10 or MALT1 signaling

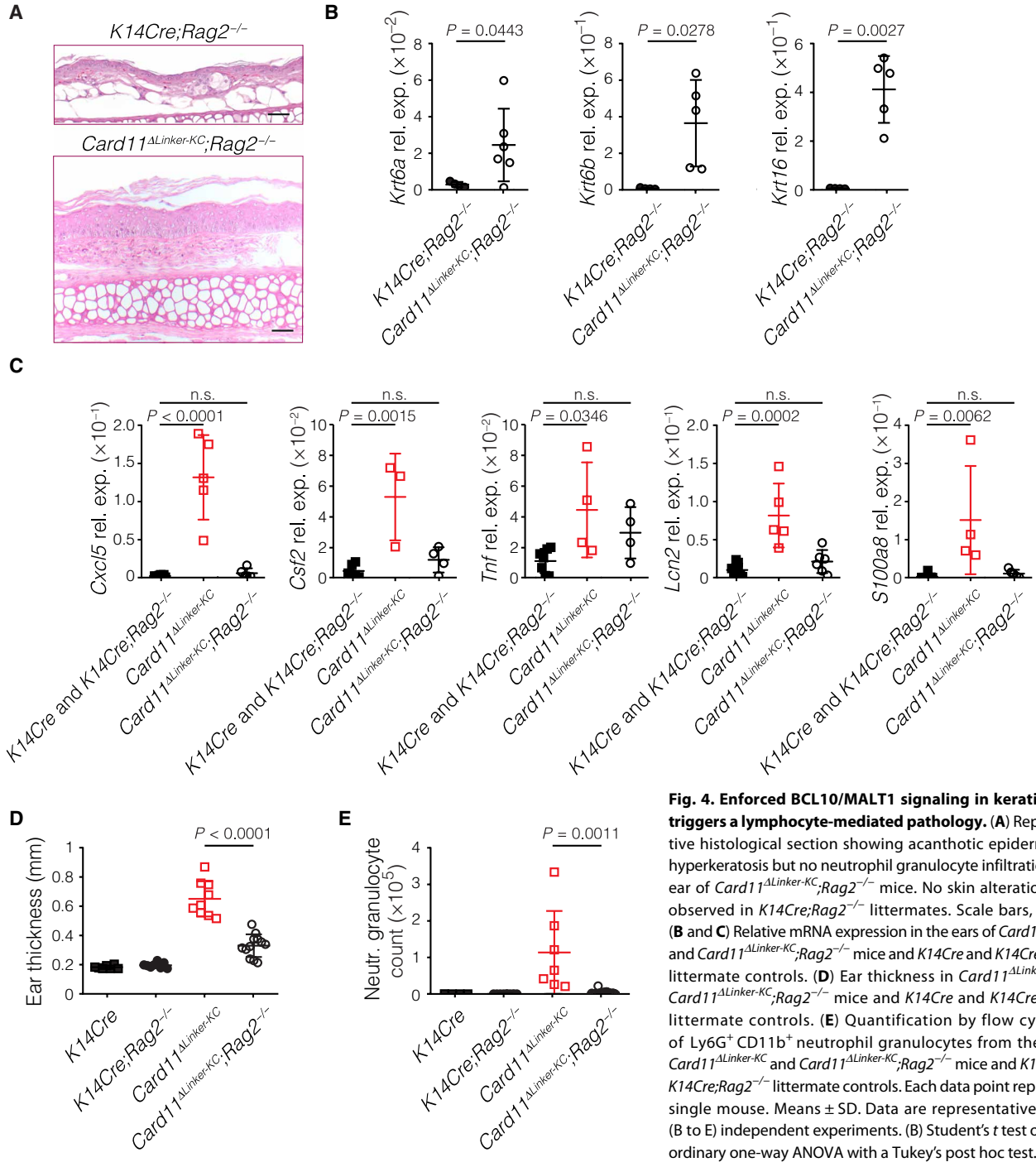

Fig. 4. Enforced BCL10/MALT1 signaling in keratinocytes triggers a lymphocyte-mediated pathology. (**A**) Representative histological section showing acanthotic epidermis with hyperkeratosis but no neutrophil granulocyte infiltration in the ear of *Card11*$^{\Delta Linker\text{-}KC}$*;Rag2*$^{-/-}$ mice. No skin alterations were observed in *K14Cre;Rag2*$^{-/-}$ littermates. Scale bars, 200 μm. (**B** and **C**) Relative mRNA expression in the ears of *Card11*$^{\Delta Linker\text{-}KC}$ and *Card11*$^{\Delta Linker\text{-}KC}$*;Rag2*$^{-/-}$ mice and *K14Cre* and *K14Cre;Rag2*$^{-/-}$ littermate controls. (**D**) Ear thickness in *Card11*$^{\Delta Linker\text{-}KC}$ and *Card11*$^{\Delta Linker\text{-}KC}$*;Rag2*$^{-/-}$ mice and *K14Cre* and *K14Cre;Rag2*$^{-/-}$ littermate controls. (**E**) Quantification by flow cytometry of Ly6G^{+} CD11b^{+} neutrophil granulocytes from the ears of *Card11*$^{\Delta Linker\text{-}KC}$ and *Card11*$^{\Delta Linker\text{-}KC}$*;Rag2*$^{-/-}$ mice and *K14Cre* and *K14Cre;Rag2*$^{-/-}$ littermate controls. Each data point represents a single mouse. Means ± SD. Data are representative of $n = 2$ (B to E) independent experiments. (B) Student's *t* test or (C to E) ordinary one-way ANOVA with a Tukey's post hoc test.

(fig. S4, H and I). The regulatory function of the BCL10/MALT1 signalosome in keratinocytes appears to be conserved between mice and humans, as the small interfering RNA (siRNA)–mediated knockdown of *BCL10* or *CARD14* in primary human keratinocytes also decreased IL-17A–induced *TNF*, *CXCL5*, and *CSF2* expressions (Fig. 5, J to M).

BCL10/MALT1 signalosomes in keratinocytes release specific negative regulators of inflammation

Because CARD14 signals together with ACT1 and TRAF6 to IL-17R–induced canonical NF-κB activation (*21*), we next explored whether BCL10 and MALT1 are also involved in the IL-17R proximal pathway. Unexpectedly, although BCL10 and MALT1 were essential for IL-17A–induced cytokine production (Fig. 5, B to I), both proteins were completely dispensable for IL-17A–induced IKK activation, for subsequent IκBα phosphorylation and for NF-κB p65 phosphorylation (Fig. 6, A and B). In addition, we also observed normal IL-17A–induced p38 and JNK kinase activation in *Bcl10*- and *Malt1*-deficient keratinocytes (Fig. 6, A and B). Likewise, although the BCL10/MALT1 complex controlled IL-1β– and TNF-induced cytokine responses in keratinocytes (Fig. 5, B to I), BCL10 was dispensable for IL-1β– and TNF-induced IKK activation, IκBα phosphorylation and NF-κB p65 phosphorylation, as well as p38 and JNK activation (Fig. 6, C and D). Thus, the BCL10/MALT1 signalosome is not involved in IL-17R–, IL-1R–, or TNF receptor–induced proximal events that lead to canonical NF-κB, JNK, or p38 activation.

To define the specific roles of BCL10 in keratinocyte responses, we next performed RNA sequencing (RNA-seq) analysis of *Bcl10*-proficient and *Bcl10*-deficient keratinocytes after IL-17A stimulation. First, we created an IL-17A response gene signature using a list of genes that are up-regulated by IL-17A stimulation of normal human keratinocytes (*43*), which we termed *IL17_NHEK*. As expected, IL-17A stimulation induced significant enrichment of this IL17_NHEK signature in both $Bcl10^{+/-}$ and $Bcl10^{-/-}$ murine keratinocytes, as shown by gene set enrichment analysis (GSEA) (Fig. 6E and fig. S5A). However, direct comparison of $Bcl10^{+/-}$ and $Bcl10^{-/-}$ keratinocytes demonstrated a stronger enrichment of IL17_NHEK in *Bcl10* competent keratinocytes than in *Bcl10*-deficient cells (Fig. 6F and fig. S5B), demonstrating that BCL10 is required for full expression of the keratinocyte IL-17 response.

Because BCL10/MALT1 complexes can, in principle, amplify signals from inflammatory pathways by inactivating the negative inflammatory regulators A20 (*44*) and CYLD (*45*) in multiple cell types, we next studied the proteolytic processing of these MALT1 substrates in primary murine keratinocytes. In line with published data (*46*), we observed constitutive processing of both A20 and CYLD in wild-type keratinocytes, as demonstrated by faster-migrating specific bands in Western blots (Fig. 6, G and H). Although A20 and CYLD processing was not further enhanced by IL-17A stimulation, it was absent in *Bcl10*- and *Malt1*-deficient keratinocytes (Fig. 6, G and H), indicating that A20 and CYLD processing was mediated by MALT1 protease activity. Consistent with this hypothesis, enforced activation of BCL10/MALT1 signaling in $Card11^{\Delta Linker\text{-}KC}$ keratinocytes enhanced A20 and CYLD cleavage (Fig. 6I). Furthermore, we also detected MALT1-mediated, constitutive proteolytic processing of the MALT1 substrate RelB (*47*) (fig. S5C). Regnase-1 is an additional MALT1 substrate in lymphocytes (*48*). IL-17A stimulation of $Bcl10^{-/-}$ and $Malt1^{-/-}$ keratinocytes induced normal degradation of Regnase-1 (Fig. 6, J and K), which was previously demonstrated to be induced by IKK-mediated Regnase-1 phosphorylation (*49*). Moreover, the absence of keratinocyte BCL10/MALT1 complexes allowed regular induction of the IL-17A target gene *Nfkbiz* (fig. S4, D and E), further indicating that the BCL10/MALT1 complex controls only selective keratinocyte responses to cytokines.

To directly evaluate whether the failure to inactivate negative regulators of inflammation underlies the decreased cytokine production in *Bcl10*- or *Malt1*-deficient keratinocytes, we next inactivated the stabilized A20 in $Bcl10^{-/-}$ keratinocytes using RNA interference (Fig. 7A). siRNA-mediated A20 inactivation allowed normal IL-17A–induced *Cxcl5* and *Csf2* expression in *Bcl10*-deficient keratinocytes and increased the expression of *Tnf* (Fig. 7, B to D). This effect was however not due to altered expression of *Il17ra* and *Traf3ip2* (encoding for ACT1) because their expression was not altered by the presence of BCL10 or A20 (fig. S6, A and B). Furthermore, not all IL-17A responses were affected, as BCL10-independent induction of *Nfkbiz* was not increased upon A20 siRNA treatment (Fig. 7E).

Next, we used keratinocytes from an additional knock-in mouse line that harbors a point mutation in the MALT1 catalytic domain (*Malt1 paracaspase-mutant* or $Malt1^{PM}$ mice), in which the MALT1 protein is expressed from the endogenous *Malt1* locus at normal levels and is able to assemble into BCL10/MALT1 complexes but is specifically impaired in its proteolytic functioning (*50*). Keratinocytes from $Malt1^{PM/-}$ mice showed severely diminished up-regulation of *Tnf*, *Cxcl5*, and *Csf2* upon IL-17A stimulation (Fig. 7, F to H), demonstrating on a genetic level that the proteolytic function of MALT1 is key for the keratinocyte inflammatory response.

To explore the role of the MALT1 protease in the increased cytokine responses in keratinocytes with activated BCL10/MALT1 signaling, we then pharmacologically inhibited the MALT1 proteolytic function in $Card11^{\Delta Linker\text{-}KC}$ keratinocytes with mepazine (*51*, *52*). Mepazine treatment led to diminished IL-17A–induced *Tnf*, *Cxcl5*, and *Csf2* expressions but did not interfere with the up-regulation of *Nfkbiz* (fig. S6, C to F). A comparable effect was observed in mepazine-treated $Card14^{\Delta E138}$ keratinocytes (fig. S6, G to J). Last, to study the keratinocyte-intrinsic functions of the MALT1 protease in skin inflammation in vivo, we engineered mice that expressed protease-mutated MALT1 together with $CARD11^{\Delta Linker}$ only in keratinocytes but not in other cell types ($Card11^{\Delta Linker\text{-}KC}$;$Malt1^{PM\text{-}KC}$ mice). Keratinocyte-intrinsic MALT1 protease inactivation strongly attenuated psoriasiform skin inflammation, as $Card11^{\Delta Linker\text{-}KC}$;$Malt1^{PM\text{-}KC}$ mice exhibited significantly reduced ear swelling (Fig. 7I), local inflammatory cytokine production (Fig. 7J), and neutrophil infiltration (Fig. 7K).

Keratinocyte BCL10/MALT1 signalosomes are active in sporadic psoriasis

Overall, our analysis in clean genetic mouse models established essential keratinocyte-intrinsic functions of BCL10/MALT1 signaling in inflammatory responses beyond putative selective effects of inherited *CARD14-GOF* alterations in the IL-17R proximal pathway. Because these BCL10/MALT1-mediated functions are required for the amplification of multiple inflammatory signals and sufficient to drive psoriasiform skin inflammation, we speculated that keratinocyte BCL10/MALT1 signaling could also play a broader role in human sporadic psoriasis. To explore this hypothesis in primary human psoriasis skin specimens, we first established a transcriptomic signature of BCL10/MALT1 activation (Fig. 8A). To this end, we performed RNA-seq in murine keratinocytes with genetically enforced

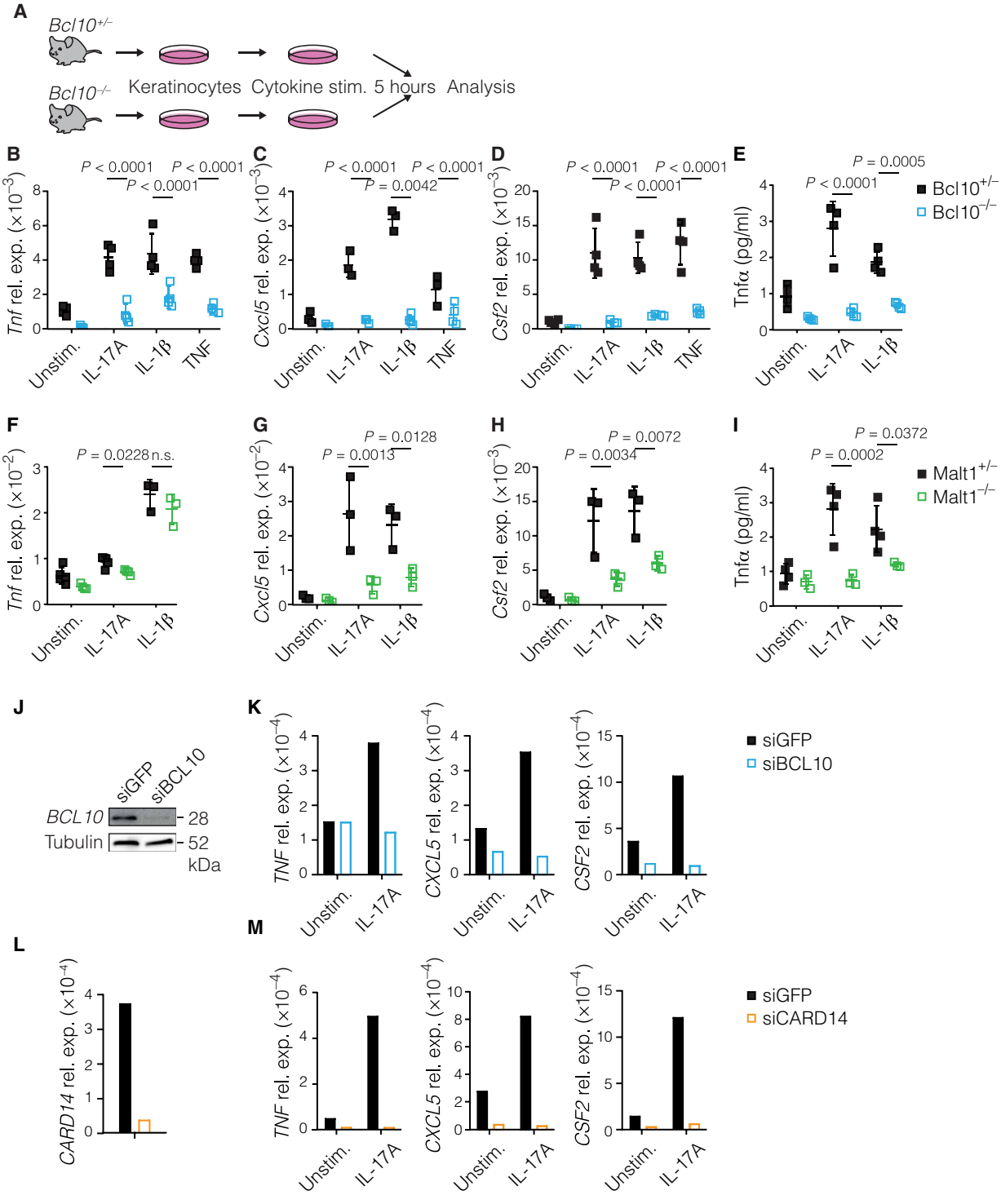

Fig. 5. BCL10/MALT1 signaling in keratinocytes amplifies secondary cytokine circuits. (**A**) Keratinocytes were isolated from newborn *Bcl10*$^{+/-}$ and *Bcl10*$^{-/-}$ mice, cultured and stimulated with the indicated cytokine for 5 hours. (**B** to **I**) (B to D and F to H) Relative mRNA expression and (E and I) cytokine secretion in keratinocytes isolated from (B to E) *Bcl10*$^{+/-}$ and *Bcl10*$^{-/-}$ (F to I) or *Malt1*$^{+/-}$ and *Malt1*$^{-/-}$ mice and stimulated for 5 hours with the indicated cytokines. (**J**) Western blotting of normal human epidermal keratinocytes treated with siRNAs against *BCL10* or *GFP* for 72 hours (*GFP* served as a control). (**K**) Relative mRNA expression in normal human epidermal keratinocytes treated with siRNAs against *BCL10* or *GFP* for 72 hours and stimulated with IL-17A for 5 hours. (**L** and **M**) Relative mRNA expression in normal human epidermal keratinocytes treated with siRNAs against *CARD14* or *GAPDH* for 72 hours and stimulated with IL-17A for 5 hours (*GAPDH* served as a control). (B to I) Each data point represents a single mouse. Means ± SD. Two-way ANOVA with Sidak's post hoc test. (B to I, L, and M) The data are representative of $n = 2$ independent experiments. (J and K) Data are representative of $n = 3$ independent experiments.

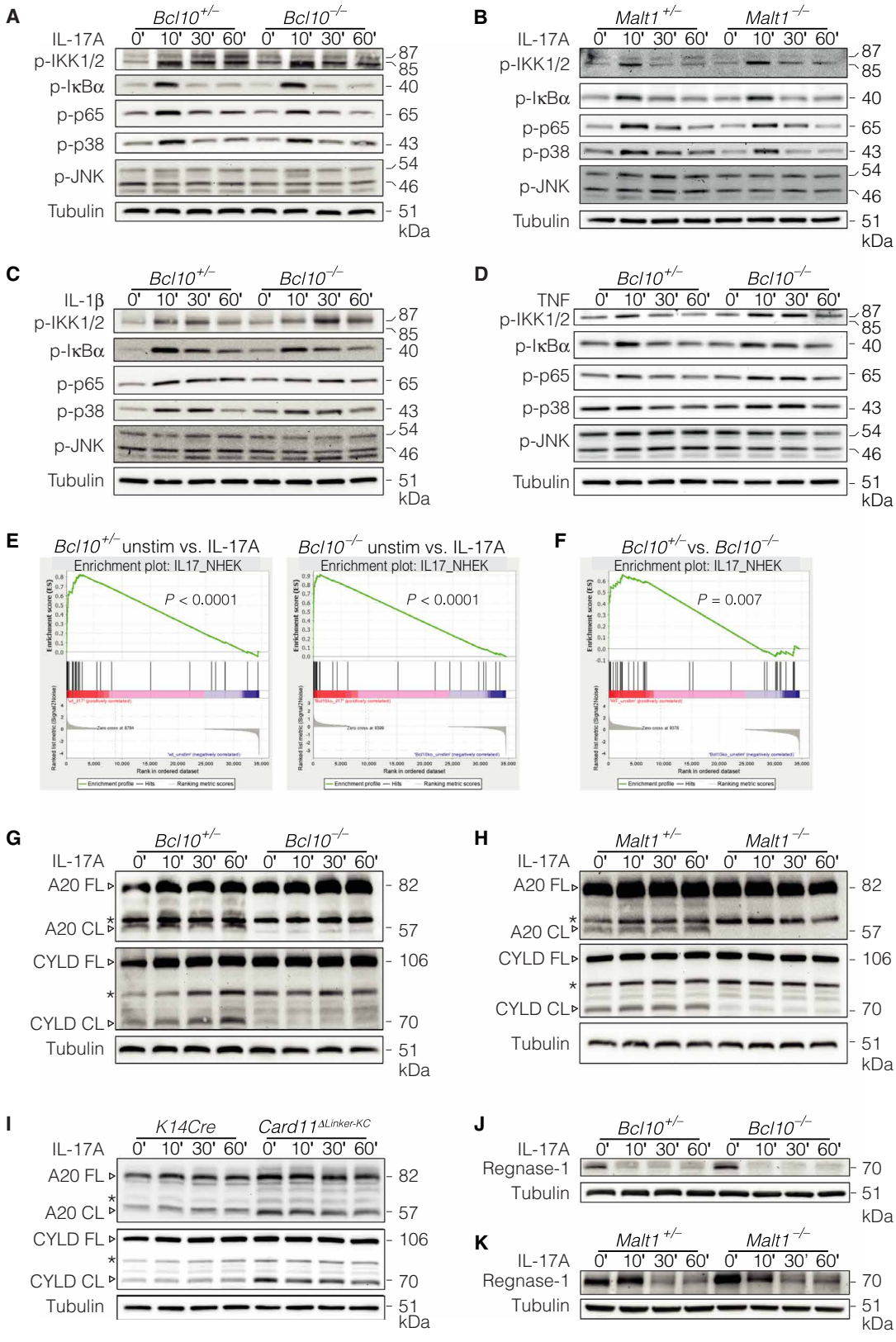

Fig. 6. BCL10/MALT1 signalosomes in keratinocytes inhibit specific negative regulators of inflammation. (**A** to **D** and **G** to **K**) Western blotting of keratinocytes isolated from (A, C, D, G, and J) *Bcl10*$^{+/-}$ and *Bcl10*$^{-/-}$, (B, H, and K) *Malt1*$^{+/-}$ and *Malt1*$^{-/-}$ or (I) *K14Cre* and *Card11*$^{\Delta Linker\text{-}KC}$ mice and stimulated with (A and B and G to K) IL-17A, (C) IL-1β, or (D) TNF for the indicated time points. (**E** and **F**) Keratinocytes were isolated from *Bcl10*$^{+/-}$ ($n = 2$) and *Bcl10*$^{-/-}$ ($n = 3$) mice and left unstimulated or stimulated for 5 hours with IL-17A. (E) Gene set enrichment analysis of the NHEK_IL17 gene set in unstimulated versus IL17A-stimulated, (left) *Bcl10*$^{+/-}$ and (right) *Bcl10*$^{-/-}$ keratinocytes (F) as well as in *Bcl10*$^{+/-}$ versus *Bcl10*$^{-/-}$ keratinocytes. The NHEK_IL17 gene set consists of genes up-regulated upon IL-17A stimulation in normal human keratinocytes (*43*). (A to D and G to K) Data are representative of $n = 3$ independent experiments. FL, full length; CL, cleaved. * indicates nonspecific bands.

(CARD11$^{\Delta Linker}$-driven) BCL10/MALT1 activity and in wild-type keratinocytes. We termed the set of 293 significantly up-regulated genes [$\log_2$ fold change > 1.5 and false discovery rate (FDR) < 0.05] that were induced by BCL10/MALT1 activity *BM_activation_KC_UP* (Fig. 8A). Using this signature for single sample GSEA on ca. 800 human cell lines (fig. S7, A to C), we found that although *Bcl10* itself was not part of the 293 genes defining *BM_activation_KC_UP*, *BCL10* expression positively correlated with *BM_activation_KC_UP* in this large dataset. Therefore, we first analyzed *BCL10* mRNA expression in three independent transcriptomic datasets from human psoriatic lesional skin and healthy donor skin (Fig. 8B). We detected significantly higher *BCL10* expression in psoriatic skin than in healthy skin in all three datasets (Fig. 8C). Moreover, upon comparing transcriptomes from paired lesional and nonlesional skin samples of patients with sporadic psoriasis in three additional datasets (Fig. 8D), *BCL10* gene expression was significantly higher in the lesional than

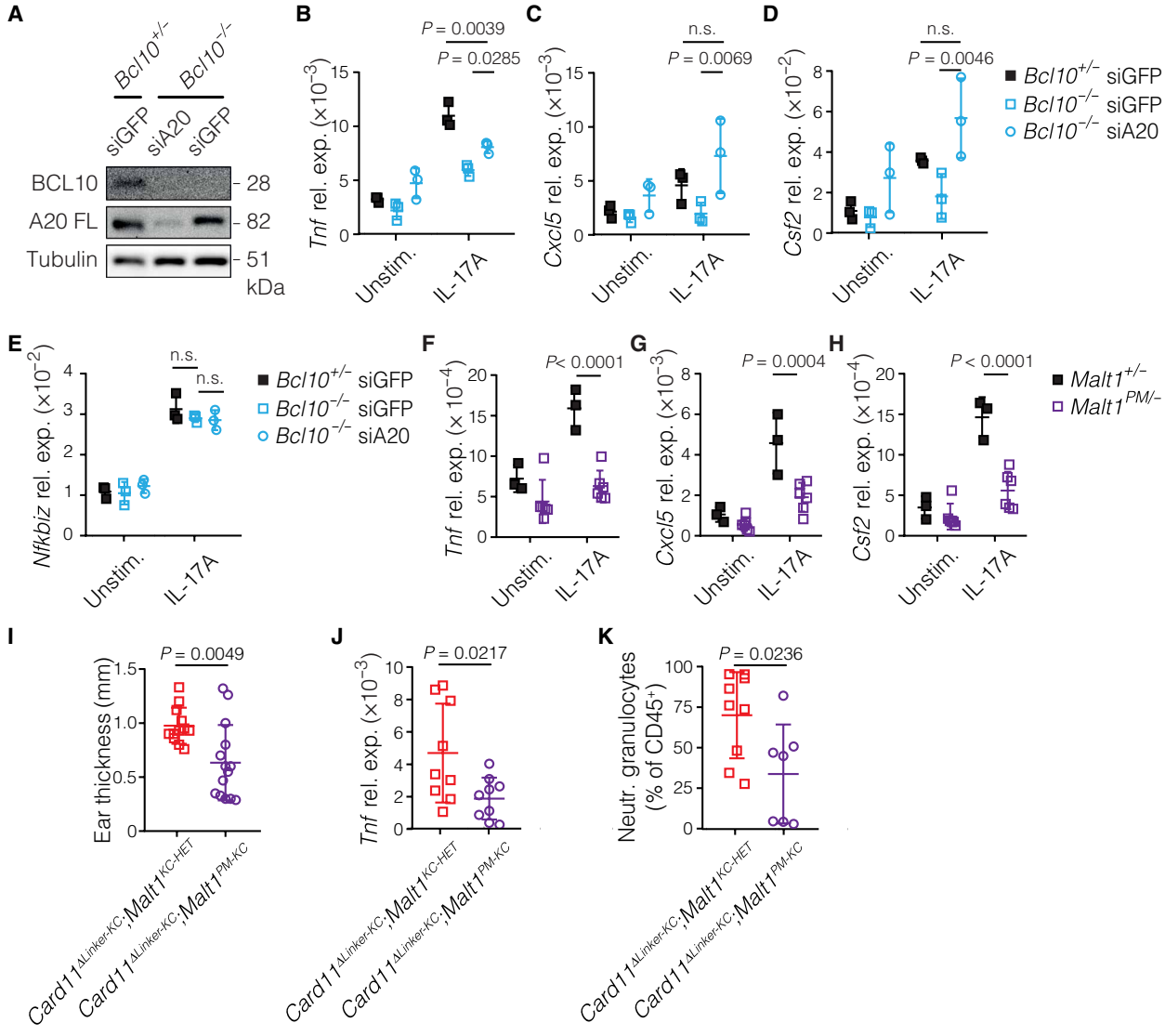

Fig. 7. MALT1 paracaspase facilitates keratinocyte inflammatory responses by cleaving negative regulators and thus controls the magnitude of keratinocyte cytokine responses. (**A**) Western blotting of keratinocytes isolated from *Bcl10*$^{+/-}$ and *Bcl10*$^{-/-}$ mice and treated with siRNAs against *A20* or *GFP* for 72 hours (GFP served as a control).(**B** to **E**) Relative mRNA expression in keratinocytes isolated from *Bcl10*$^{+/-}$ and *Bcl10*$^{-/-}$ mice and treated with siRNAs against *A20* or *GFP* for 72 hours and stimulated with IL-17A for 5 hours. (**F** to **H**) Relative mRNA expression in keratinocytes isolated from *Malt1*$^{+/-}$ and *Malt1*$^{PM/-}$ mice and stimulated for 5 hours with IL-17A. (**I** and **J**) (I) Ear thickness and (J) relative mRNA expression in the ears of *Card11*$^{\Delta Linker\text{-}KC}$;*Malt1*$^{KC\text{-}HET}$ and *Card11*$^{\Delta Linker\text{-}KC}$;*Malt1*$^{PM\text{-}KC}$ mice. (**K**) Quantification by flow cytometry of Ly6G^{+} CD11b^{+} neutrophil granulocytes from the ears of *Card11*$^{\Delta Linker\text{-}KC}$;*Malt1*$^{KC\text{-}HET}$ and *Card11*$^{\Delta Linker\text{-}KC}$;*Malt1*$^{PM\text{-}KC}$ mice. Each data point represents a single mouse. Means ± SD. (A to H, J, and K) Data are representative of $n = 2$ independent experiments. (B to H) Two-way ANOVA with Sidak's post hoc test or (I to K) Student's *t* test.

in the nonlesional skin (Fig. 8E). Next, we studied BCL10 protein expression in a series of skin samples from patients with sporadic psoriasis using immunohistochemistry. BCL10 protein expression was significantly increased in lesional epidermal keratinocytes compared with paired nonlesional epidermal keratinocytes (Fig. 8, F and G). Moreover, we also found significantly increased *MALT1* expression in psoriatic skin compared with healthy control skin (fig. S8A), as well as in psoriatic lesional skin compared with the paired nonlesional skin of patients with sporadic psoriasis (fig. S8B). Encouraged by these results, we next performed GSEA with the *BM_activation_KC_UP* gene signature in human sporadic psoriasis. A significant positive enrichment of *BM_activation_KC_UP* was observed in psoriatic lesional skin in comparison with healthy donor skin in the investigated datasets (Fig. 8H).

Functional annotation of the 293 target genes of enforced BCL10/MALT1 signaling in keratinocytes (Fig. 8A) revealed a significant positive enrichment (FDR < 0.1) of nine KEGG (Kyoto Encyclopedia of Genes and Genomes) pathways, which included TNF, TLR, and chemokine signaling pathways, as well as molecular pathways induced by various viruses (table S1). Eight of these nine BCL10/MALT1-triggered KEGG signatures were previously established as bona fide characteristics of human psoriatic skin lesions (Fig. 8I) (*53*). Conversely, GSEA with the significantly enriched KEGG pathways in human lesional psoriatic skin (*53*) revealed that 10 of the

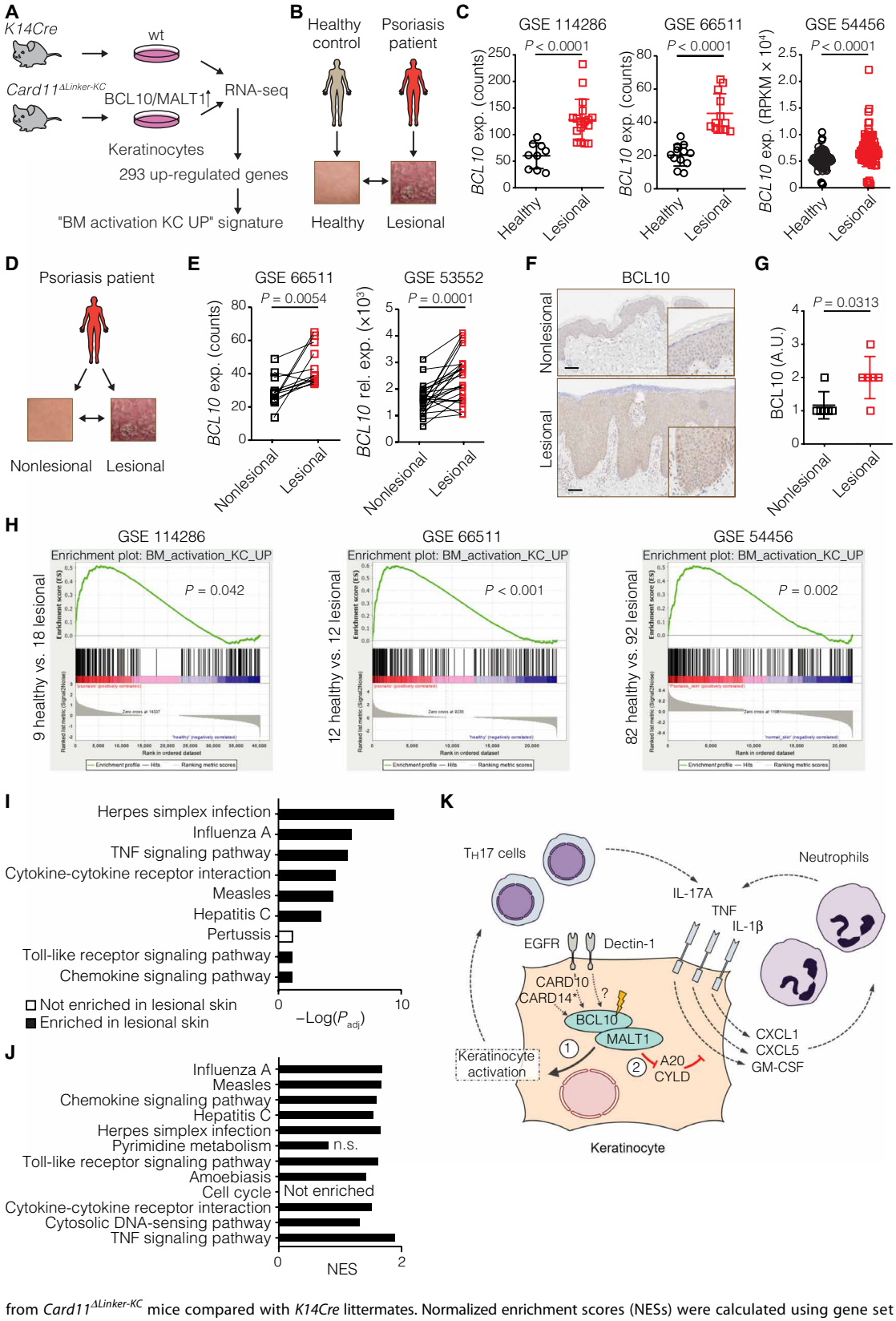

Fig. 8. Keratinocyte BCL10/MALT1 signalosomes are active in sporadic human psoriasis. (**A**) Keratinocytes were isolated from newborn *K14Cre* and *Card11*$^{\Delta Linker\text{-}KC}$ mice, cultured and stimulated with IL-17A for 5 hours. RNA-seq analysis revealed that 293 genes were significantly (log_2 fold change > 1.5 and FDR < 0.05) up-regulated upon BCL10/MALT1 activation. These genes were used to define the BM_activation_KC_UP gene set. wt, wild type. (**B** and **C**) Three transcriptomic datasets of psoriatic lesional skin and healthy donor skin were retrieved from the Gene Expression Omnibus and analyzed for *BCL10* expression. (**D** and **E**) Two transcriptomic datasets of lesional and paired nonlesional skin of patients with sporadic psoriasis were retrieved from the Gene Expression Omnibus and analyzed for *BCL10* expression. (**F**) Representative immunohistochemical staining of BCL10 in (bottom) lesional and (top) paired nonlesional skin of a patient with sporadic psoriasis. Scale bars, 100 μm. (**G**) Quantification of BCL10 protein expression in lesional and paired nonlesional skin of patients with sporadic psoriasis. (**H**) Enrichment plot of the BM activation_KC_UP gene set in psoriatic lesional skin versus healthy donor skin. Transcriptomic datasets of psoriatic lesional skin and healthy donor skin were retrieved from the Gene Expression Omnibus. (**I**) KEGG pathways significantly enriched in differentially expressed genes (up-regulated) upon BCL10/MALT1 signaling in keratinocytes isolated from *Card11*$^{\Delta Linker\text{-}KC}$ mice compared with *K14Cre* littermates. The adjusted significance of enrichment was calculated using the DAVID online tool. KEGG pathways with black bars are significantly enriched in psoriatic lesional versus nonlesional skin (*53*). (**J**) KEGG pathways enriched in human psoriatic lesional versus nonlesional skin (*53*) are also enriched in keratinocytes isolated from *Card11*$^{\Delta Linker\text{-}KC}$ mice compared with *K14Cre* littermates. Normalized enrichment scores (NESs) were calculated using gene set enrichment analysis. (**K**) Schematic view of the role of keratinocyte BCL10/MALT1 signaling in psoriatic inflammation. (C, E, and G) Each data point represents a patient sample. Means ± SD. (C) Student's *t* test, (E) paired Student's *t* test, or (G) Wilcoxon one-sided, matched pairs signed rank test. RPKM, reads per kilobase per million mapped reads. GM-CSF, granulocyte-macrophage colony-stimulating factor.

12 pathways with murine counterparts were also enriched upon enforced BCL10/MALT1 signaling in murine CARD11$^{\Delta Linker}$-expressing keratinocytes (Fig. 8K). Together, these results provide the first indications of aberrant BCL10/MALT1 signaling in lesional keratinocytes from sporadic human patients with psoriasis.

DISCUSSION

Activating *CARD14* mutations are found in rare cases of patients with familial psoriasis and pityriasis rubra pilaris (*7*, *9*–*11*), and respective mutations in the mouse germline (*19*–*21*) or in keratinocytes (*22*) are sufficient to drive psoriasiform skin inflammation in vivo with characteristics of the human disease psoriasis. By conditionally deleting *Bcl10* or *Malt1* only in keratinocytes in germline mutant mice that harbor pathogenic *Card14*$^{\Delta E138}$ mutation in all cell types, we unequivocally demonstrate that the keratinocyte-intrinsic function of the BCL10/MALT1 complex is absolutely essential to drive CARD14-GOF–induced skin inflammation. Thus, aberrant signaling in other putatively CARD14-expressing cell types—such as Langerhans cells, dermal γδ T cells, or dermal endothelial cells—is largely negligible for the pathogenesis of this severe inherited disorder.

Because CARD14 can signal together with TRAF6 and ACT1 in the IL-17R proximal pathway (*21*), disease-associated CARD14 variants have been considered a pathophysiological link between psoriatic IL-17A stimulation and inflammatory IKK-mediated NF-κB activation (*17*, *21*, *23*). We now provide the first molecular evidence that BCL10 and MALT1, in contrast to CARD14 (*21*), are not involved in the IL-17R proximal TRAF6/ACT1 cascade because IL-17A stimulation of primary *Bcl10*- or *Malt1*-deficient keratinocytes triggers regular IKK activation and normal IκBα phosphorylation and degradation. Likewise, IL-17A–induced mitogen-activated protein kinase (MAPK) signaling, which is defective in *Card14*$^{-/-}$ keratinocytes (*21*), is also intact in *Bcl10*$^{-/-}$ or *Malt1*$^{-/-}$ keratinocytes. In contrast, our study reveals a much more pleiotropic role for BCL10/MALT1 complexes in keratinocyte inflammatory signaling, as these complexes strongly amplify pathophysiological outputs from a series of psoriasis-relevant cytokines, including not only IL-17A but also IL-1β and TNF, and potentially others by releasing A20 and CYLD inhibition, presumably in the proximity of cytokine-activated inflammatory signalosomes. Consistent with this model, the blunted inflammatory responses in *Bcl10*-deficient keratinocytes could be restored by inactivating A20. A20 and CYLD have previously been established as bona fide MALT1 proteolytic targets (*44*, *45*), and A20 and its interacting protein TNIP1 (also known as ABIN1) (*3*) as well as CYLD are also located within genetic loci associated with psoriasis susceptibility (*54*). Moreover, epidermal loss of A20 or TNIP1 facilitates psoriasiform inflammation in mice (*55*, *56*) even in the absence of *CARD14* mutations.

In addition to demonstrating an intrinsic requirement of BCL10/MALT1 signaling and protease activity for keratinocyte inflammatory responses, we also provide conclusive genetic evidence that the selective keratinocyte-intrinsic enforcement of BCL10/MALT1 activity with an artificial CARD11$^{\Delta Linker}$ engager molecule is sufficient to drive psoriasiform skin inflammation that features the key characteristics of the human disease on a histopathological, cellular, and molecular signature level. Thus, BCL10/MALT1 signalosomes themselves can in principle function at the origin of the psoriatic inflammatory cascade. On the basis of our genetic findings in conditional knock-in and knockout mice in the presence or absence of lymphocytes (*Rag2*$^{-/-}$), we propose two distinct functions for BCL10/MALT1 signalosomes within keratinocytes in psoriasis (summarized in Fig. 8K). First, pathological activation of BCL10/MALT1 signaling within keratinocytes can provoke acanthosis and hyperkeratosis and trigger inflammatory responses with cell-autonomous NF-κB activation and high levels of inflammatory cytokine production. Subsequently, these events can promote a T_H17-dominated lymphocytic reaction. Although acanthosis and hyperkeratosis are also detected in the absence of inflammatory leukocytes, the presence and recruitment of lymphocytes and the production of IL-17A—presumably by infiltrating αβ T cells—are required to drive psoriasiform skin inflammation and maintain the full phenotype, as the pathology does not develop in a *Rag2*-deficient background and is strongly ameliorated by treatment with anti–IL-17A. These data are further corroborated by the findings that the psoriasiform phenotype of different *Card14-GOF* mouse models is also reversed upon IL-23 or IL-17A blockade (*19*, *21*). Moreover, in the presence of lymphocyte-mediated inflammatory conditions, the keratinocyte-intrinsic BCL10/MALT1 complex has a second key function, as it inactivates inhibitory factors such as A20 and CYLD through MALT1 protease activity. Therefore, the BCL10/MALT1 signalosome licenses pathogenic keratinocytes to fully respond to multiple exogenous inflammatory stimuli, such as IL-17A, IL-1β, or TNF, with potent production of additional cytokines and chemokines that subsequently attract and stimulate neutrophils to propel a vicious cycle to exaggerate debilitating skin disorders.

On the basis of this model, we speculated that BCL10/MALT1 signaling could have a broader role in psoriasis beyond rare familial *CARD14-GOF*–associated cases (*57*). This hypothesis is supported by enhanced *BCL10* and *MALT1* gene expression in lesional compared with nonlesional skin from patients with sporadic psoriasis, which positively correlates with BCL10/MALT1 activity in a large series of human cell lines. On the basis of in silico prediction, the promoter region of *BCL10* contains binding sites for the NF-κB transcription factor p65 (*58*), which is highly active in the lesional psoriatic skin (*59*). Therefore, we speculate that the increase in *BCL10* in the lesional psoriatic skin might be mediated via NF-κB/p65 activity, potentially in a positive-feedback loop. In addition, and more importantly, transcriptomic profiling of human psoriatic lesional skin also revealed an intriguing enrichment of the pathogenic BCL10/MALT1-triggered gene expression signature, which is characterized by the specific activation of most of the established hallmark KEGG signatures of psoriasis (*53*). Together, these data suggest that uncharacterized environmental and host factors might pathologically activate keratinocyte-intrinsic BCL10/MALT1 complexes in psoriasis to promote pathological cross-talk between a damaged or stressed epidermis and the immune system during the initiation and/or amplification of skin inflammation. Because keratinocytes can respond to fungal cell wall components or pathogen-associated molecular patterns from *Staphylococcus aureus* with the activation of BCL10/MALT1 signaling in response to innate immune receptor triggering (*26*) and furthermore express, in addition to CARD14, its homolog CARD10 (*46*), which can induce BCL0/MALT1 activity upon the stimulation of G protein–coupled or growth factor receptors (*46*), it is conceivable that such BCL10/MALT1 activators could be of either microbial or sterile origin. While these factors need to be defined in future studies, the bacterial and fungal microbiomes could play an instigating function in the stimulation of these pathways, as there is considerable evidence that alterations in the skin microbiome could play a decisive role in the

pathogenesis of psoriasis (*60*) and that the yeast *Malassezia furfur* is more abundant in psoriatic skin than in healthy skin (*61*, *62*). In addition to rare CARD14-GOF variants, common variants have also been associated with sporadic psoriasis (*57*). Nevertheless, in vitro studies of common variants have so far failed to demonstrate increased activity (*57*). Therefore, whether these variants contribute to the observed activation of BCL10/MALT1 complexes in lesional psoriatic skin needs to be further investigated.

In conclusion, rare, monogenic diseases have frequently provided key insights into biological pathways that enhance our understanding of common complex traits. Although activating *CARD14-GOF* mutations are found in individual cases of familial inflammatory skin diseases, they not only signal via TRAF6/ACT1 in the IL-17R pathway but also interact with BCL10 and MALT1 and trigger the activation of BCL10/MALT1 signaling with NF-κB and paracaspase activation (*18*, *22*, *25*, *26*). By mechanistically demonstrating in clean genetic models that BCL10/MALT1 complexes play a more general role in inflammatory keratinocyte signaling, our data provide a rationale to further explore the mechanisms and consequences of keratinocyte BCL10/MALT1 signaling in sporadic psoriasis. Because MALT1 protease activity is critical for inflammatory keratinocyte responses and MALT1 protease inhibitors are in preclinical and clinical development for lymphoma treatment (ClinicalTrials.gov Identifier: NCT03900598), our study also recommends to explore the utility of such inhibitors for the treatment of sporadic psoriasis.

MATERIALS AND METHODS

Study design

This was a preclinical and translational study on the role of keratinocyte BCL10/MALT1 complexes in psoriasiform skin inflammation. Genetically engineered mice were crossed, and the resulting skin phenotype was characterized by measurement of ear thickness and gene expression, histopathological examination, and flow cytometric evaluation of infiltrating immune cells. Mice of both sexes, newborn or aged 8 to 16 weeks, were used for all experiments. Littermate controls were used whenever possible. For in vitro experiments, keratinocytes were isolated from newborn mice, cultured and stimulated with cytokines, followed by gene expression analysis and cytokine beads assays. *Rosa26*$^{LSL\text{-}Card11\Delta Linker}$ mice contain the cDNA of a constitutive active variant of the murine *Card11* gene (the linker domain was excised) in the ubiquitously expressed *Rosa26* gene locus. For the transcriptional analysis of human skin samples, publicly available datasets of the skin samples of patients with psoriasis and healthy donors from the Gene Expression Omnibus were used. For the immune histology, skin samples of patients with psoriasis treated at the Department of Dermatology at the Technical University of Munich were analyzed.

Mice

For the generation of *Rosa26*$^{LSL\text{-}Card11\Delta Linker}$ mice, the cDNA of the murine *Card11* gene without the linker domain (*32*) was cloned into a Rosa26-targeting vector (*63*), in which it was preceded by loxP-STOP-loxP sequences to allow for conditional expression (fig. S2A), and followed by the cDNA sequence of enhanced GFP. The targeting vector was linearized and electroporated into E14K murine embryonic stem cells, followed by clone selection. The clones were analyzed for homologous recombination by Southern blotting using a 5′-flanking Rosa26 probe of the following sequence: 5′-gat caa aac act aat gaa ctt taa gtc ctg tga agg gta aaa cct cag ata gta aca aaa agc ttc caa ccc ctc ctc aaa caa aaa acc cca agt ctt taa ctt tga tcc agt ttt cag atg ctg ata tcc ata aat gga tac agt tat gaa ttg cta att ctg gtc tct tca cta gca aaa agc aaa gca gct cag cag tac aat ttc cca gga aag caa gca agg ttt ctt tcc agc ctg agc agc cat cac taa gtg cag ttc cct gca gcc aac agc att aat gga cgc tgc act gct gtc ctt ccc tgg aga cag cag cca gca cta ctc aag ctt ctc acg tag caa cca gag ctc cag agc cag cag ctg ctg ccg cct tgt ata ctc act cct gtg atc caa cac agg agc aac ctt ttc ttt acc cca ccc cca ctt ctt aac aca ctt ttt ttt ggg ggg ggg ggg gaa caa gtg ctc cat gct gga agg att gga act atg ctt tta gaa agg aac aat cct aag gtc act ttt aaa ttg agg tct ttg att tga aaa tca aca aat acc aaa ttc caa ata ttc gtt tta att aa-3′ (fig. S2B) (*64*). The blastocyst injection of the clones (performed by PolyGene) and subsequent chimera breeding resulted in *Rosa26*$^{LSL\text{-}Card11\Delta Linker}$ mice.

Bcl10$^{-/-}$, *Malt1*$^{-/-}$, *Bcl10*^{floxed}, *Malt1*^{floxed}, and *Malt1*^{PM} mice have been previously described (*27*, *39*, *40*, *50*). To conditionally ablate and/or express genes in epithelial cells, *K14Cre* mice (*28*) were used, which were purchased from the Jackson Laboratory [Tg (KRT14-cre) 1Amc/J]. *Rag2*$^{-/-}$ and *Card14*$^{\Delta E138}$ mice were also obtained from the Jackson Laboratory [B6(Cg)-Rag2$^{tm1.1Cgn/J}$ and C57BL/6 J-Card14^{em9Lutzy}/J] (*19*, *35*).

Experimentally induced psoriasis-like dermatitis and neutralization of IL-17A

Aldara (5% imiquimod) cream (50 mg and 5 mg) was applied to Nair crème–treated dorsal skin and ears of 8- to 9-week-old mice daily for 5 days, respectively. Control mice were treated with Nair and Vaseline crème. The ear and dorsal skin thicknesses were measured using a digital micrometer. The mice were sacrificed on day 6. For the antibody-blocking experiments, 200 μg of anti–IL-17A (Novartis) or 200 μg of anti–ciclosporin A control antibody was injected intraperitoneally into 12-week-old mice every other day for 2 weeks. Mice were randomized in all in vivo experiments. The mice were euthanized on day 14.

Analysis with flow cytometry

For single-cell suspensions derived from skin, the dorsal and ventral parts of the ears were separated. The ear skin halves and dorsal skin were then processed as previously described (*65*). They were briefly digested with dispase II (Sigma-Aldrich) and then with collagenase and deoxyribonuclease I (both from Roche) and filtered through a 70-μm nylon mesh. Cell suspensions were separated using Percoll density gradient centrifugation. For intracellular cytokine staining, cells were stimulated with phorbol 12-myristate 13-acetate (80 ng/ml) and ionomycin (1 μM; both from Sigma-Aldrich). One hour later, they were treated with brefeldin A (eBioscience) and incubated for 4 hours at 37°C. For the IL-17R staining, in vitro cultured keratinocytes were detached using 0.05% Trypsin-EDTA (Gibco). The cells were stained with a fixable viability dye (eBioscience) and the following antibodies for flow cytometric analysis: CD3ε (145-2C11, #25-0031-82), CD4 (GK1.5, #11-0041-82), CD8a (53-6.7, #45-0081-82), CD11b (M1/70, #48-0112-82), CD45 (30-F11, #48-0451-82, and #45-0451-82), CD217/IL-17Ra (PAJ-17R, #17-7182-82), IL-17A (eBio17B7, #12-7177-81), Ly6G (1A8, #12-9668-82), T cell receptor β (TCRβ) (H57-597, #47-5961-82), and TCRγδ (GL3, #17-5711-82, all from eBioscience). The data were collected with a FACSCanto II cytometer (BD Biosciences) and analyzed using FlowJo software (Tree Star).

Histology

Mouse ear biopsy specimens were fixed with 10% phosphate-buffered formalin, embedded in paraffin, and stained with hematoxylin and eosin according to standard procedures. Immunohistochemistry of human skin biopsy specimens was performed with anti-BCL10 (331.3, Santa Cruz Biotechnology) antibody using a Bond RXm (Leica, Wetzlar, Germany) system with a Polymer Refine Detection System. The psoriasis scores were evaluated according to Baker *et al.* (*33*).

Quantitative reverse transcription PCR

RNA was isolated from the ear and dorsal skin of mice using TRIzol (Invitrogen) and from cultured cells using RLT buffer from an RNeasy kit (QIAGEN). cDNA was generated using a QScript cDNA synthesis kit (QuantaBio), and quantitative real-time polymerase chain reaction (PCR) was performed using Takyon No ROX SYBR 2X MasterMix (Eurogentec) on a LightCycler Instrument II (Roche). All murine and human PCR data were normalized to the *Gapdh* and *RPLP0* values, respectively. Primer sequences used are the followings (5′ – 3′): Murine: *Gapdh* (gtg ttc cta ccc cca atg tg, ggt cct cag tgt agc cca ag), *Il17a* (atc cct caa agc tca gcg tgt c, ggg tct tca ttg cgg tgg aga g), *Il4* (ggt ctc aac ccc cag cta gt, gcc gat gat gat ctc tct caa gtg at), *Ifng* (gcc acg gca cag tca ttg a, tgc tga tgg cct gat tgt ctt); *Ccl20* (gcc tct cgt aca tac aga cgc, cca gtt ctg ctt tgg atc agc), *Csf2* (ggc ctt gga agc atg tag agg, gga gaa ctc gtt aga gac gac tt), *Cxcl1* (ccc act gca ccc aaa ccg aag, cag gtg cca tca gag cag tct gt), *Cxcl5* (gct gcc cct tcc tca gtc at, cac cgt agg gca ctg tgg ac), *Lcn2* (aca ttt gtt cca agc tcc agg gc, cat ggc gaa ctg gtt gta gtc cg), *S100a8* (aaa tca cca tgc cct cta caa g, ccc act ttt atc acc atc gca a), *Tnf* (atg agc aca gaa agc atg atc, tac agg ctt gtc act cga att), *Nfkbiz* (tgc tac aca tcc gaa gca aca, cac tgc act ctt cag gtc tgt), *Krt6a* (aga gag ggg tcg cat gaa ct, tca tct gtt aga ctg tct gcc tt), *Krt6b* (agt gcc ctg tgt acg ggg tcg tg, aca gag gta ggg agg gag gag cct), and *Krt16* (gag atc aaa gac tac agc cc, cat tct cgt act tgg tcc tg). Human: *RPLP0* (tcg aca atg gca gca tct ac, gcc ttg atg gca gca ag), *CXCL5* (tgg acg acc ttt tca agg, ctt ccc tgg gtt cag aga c), *CSF2* (tcc tga acc tga gta gag aca c, tgc tgc ttg tag tgg ctg g), *TNF* (tct tct cga acc ccg agt ga, cct ctg atg gca cga cca g), and *CARD14* (cgg gca ctt gct gga ttt g, tcc atg aga ccg cta aag tta ct).

Immunoblotting

Cells were lysed for immunoblotting in radioimmunoprecipitation assay (RIPA) buffer containing protease and phosphatase inhibitors (Calbiochem) at the indicated time points. For the detection of a RelB cleavage product, cells were pretreated with 20 μM MG132 (Sigma-Aldrich) for 60 min. The following antibodies were used: pIKK1/2 (16A6), pIκBα (5A5), pp65 (93H1), pp38 (D3F9), pJNK (81E11), BCL10 (C78F1), A20 (D13H3), RelB (C1E4), tubulin (11H10, all from Cell Signaling Technologies), CYLD (E-10, Santa Cruz Biotechnology), and Regnase-1 (MAB7875, R&D Systems).

Isolation and culture of keratinocytes

Murine keratinocytes were isolated from neonatal mice as described in Li (*66*) and cultured in calcium-free Keratinocyte SFM (Gibco) supplemented with 0.05 mM $CaCl_2$ in collagen-coated (collagen IV from human placenta, Sigma-Aldrich) flasks. Human keratinocytes were obtained from the skin of healthy individuals. The epidermis was separated from the dermis after overnight digestion with dispase (Roche Diagnostics) and then incubated in 0.05% trypsin to obtain keratinocytes, which were cultured in EpiLife medium (60 μM $CaCl_2$) supplemented with defined growth supplement (both from Thermo Fisher Scientific).

Stimulation, RNA interference, and MALT1 protease inhibition in keratinocytes

Recombinant murine IL-17A (200 ng/ml), TNF (100 ng/ml), IL-1β (10 ng/ml), and human IL-17A (50 ng/μl; all from PeproTech) were used for the stimulation experiments. For RNA interference, keratinocytes were transfected with MISSION esiRNA against A20, BCL10 or GFP (Sigma-Aldrich), or with Silencer Select siRNA against CARD14 or GAPDH (Thermo Fisher Scientific) using Lipofectamine 3000 (Thermo Fisher Scientific) 72 hours in advance of stimulation. To inhibit MALT1 paracaspase activity, cells were treated with mepazine (10 μM/ml; Sigma-Aldrich) for 6 hours before stimulation. The cells were harvested for reverse transcription PCR analysis, and the supernatants were used for cytokine bead assays 5 hours after cytokine stimulation.

Cytokine bead assay

TNF levels in cell culture supernatants were determined using the Mouse TNF Enhanced Sensitivity Flex Set Kit (BD Biosciences) according to the manufacturer's instructions. The data were collected with a FACSCanto II cytometer (BD Biosciences) and analyzed with FlowJo software (Tree Star).

NF-κB luciferase reporter assay

Keratinocytes were transfected with NF-κB luciferase reporter and PRL-TK (Promega) plasmids using Lipofectamine 3000 (Thermo Fisher Scientific). Luciferase activity was measured using the Dual-Glo Luciferase Assay System (Promega).

Transcriptome analyses

For the RNA-seq analyses, keratinocytes were isolated, cultured, and stimulated, and total RNA was isolated as described above. Library preparation from 100 ng of total RNA was performed using the NEBNext Ultra II RNA Library Prep Kit for Illumina and NEBNext Poly(A) mRNA Magnetic Isolation Module (New England Biolabs), and SE-75-base pair sequencing was performed on an Illumina NextSeq550 machine using the NextSeq 500/550 High Output Kit v2.5 cartridges (Illumina, San Diego, CA, USA). Reads were aligned to the mm10 genome using HISAT2 (*67*), and transcriptome assembly was performed using StringTie (*68*). Differential expression was assessed with Deseq2 (*69*), and the list of differentially expressed genes was defined as $\log_2$ fold change > 1.5 and FDR < 0.05. Functional annotation of differentially expressed genes was performed using DAVID software (https://david.ncifcrf.gov/) (*70*, *71*). GSEA was performed with GSEA software (*72*, *73*). The following datasets from the Gene Expression Omnibus were analyzed: GSE114286 (9 healthy controls and 18 psoriatic skin samples), GSE54456 (82 healthy controls and 92 psoriatic skin samples), GSE66511 (12 healthy controls and 12 paired psoriatic lesional and nonlesional skin samples), and GSE53552 (24 paired psoriatic lesional and nonlesional skin samples).

Correlation analysis of *BCL10* expression and CBM activation

To investigate whether *BCL10* expression correlates with the activation of BCL10/MALT1 complexes, we turned to the Cancer Cell Line Encyclopedia database, which contains transcriptomic data of 1077 human cell lines and performed single sample GSEA to look for enrichment of the BM_activation_KC_UP gene set in each cell line. Pearson's linear regression analysis was used to examine a correlation between enrichment of the BM_activation_KC_UP signature

and *Bcl10* expression. The analyzed cell lines are highly heterogeneous; therefore, the observed correlation may theoretically derive from inherent differences in *Bcl10* expression among the different cell line types. Thus, we stratified the cell lines based on their "origin" using their tgca code and reran the abovementioned analyses (fig. S7). We included gene sets of the Molecular Signatures Database containing genes up-regulated upon NF-κB activation (a direct consequence of BCL10/MALT1 activation), and we also generated a sublist of the BM_activation_KC_UP gene set by filtering for genes involved in immune functions (fig. S7C). In most, albeit not in all cell line groups, *Bcl10* expression significantly and positively correlated with the enrichment scores of both NF-κB activation and the BCL10/MALT1 activation signatures (fig. S7C).

Statistical analysis

Statistical tests were performed using GraphPad PRISM. The statistical tests are described in the respective figure legends. Error bars represent SD. $P < 0.05$ was considered statistically significant.

Study approval

Human keratinocytes were isolated from clinically healthy skin samples from patients undergoing elective operations (one 85-year-old female patient and male patients aged 78, 73, and 66 years old), while immunohistochemical staining was performed on skin samples collected from patients with psoriasis. Samples were collected at the Department of Dermatology and Allergy, Technical University of Munich upon informed consent. Ethics approval was obtained from the Institutional Review Board of the Technical University of Munich (reference number 82/19S). All work was carried out in accordance with the Declaration of Helsinki for experiments involving humans. All animal work was conducted in accordance with the German Federal Animal Protection Laws and approved by the government of Upper Bavaria (Regierung von Oberbayern, Munich, Germany, ROB-55.2-2532.Vet_02-15-26 and ROB-55.2-2532.Vet_02-19-24).

SUPPLEMENTARY MATERIALS

www.science.org/doi/10.1126/sciimmunol.abi4425
Figs. S1 to S8
Table S1
Data S1

View/request a protocol for this paper from *Bio-protocol*.

REFERENCES AND NOTES

1. C. E. Griffiths, J. N. Barker, Pathogenesis and clinical features of psoriasis. *Lancet* **370**, 263–271 (2007).
2. J. Takeshita, S. Grewal, S. M. Langan, N. N. Mehta, A. Ogdie, A. S. Van Voorhees, J. M. Gelfand, Psoriasis and comorbid diseases part I. Epidemiology. *J. Am. Acad. Dermatol.* **76**, 377–390 (2017).
3. R. P. Nair, ZK. C. Duffin, C. Helms, J. Ding, P. E. Stuart, D. Goldgar, J. E. Gudjonsson, Y. Li, T. Tejasvi, B. J. Feng, A. Ruether, S. Schreiber, M. Weichenthal, D. Gladman, P. Rahman, S. J. Schrodi, S. Prahalad, S. L. Guthery, J. Fischer, W. Liao, P.-Y. Kwok, A. Menter, G. M. Lathrop, C. A. Wise, A. B. Begovich, J. J. Voorhees, J. T. Elder, G. G. Krueger, A. M. Bowcock, G. R. Abecasis; Collaborative Association Study of Psoriasis, Genome-wide scan reveals association of psoriasis with IL-23 and NF-κB pathways. *Nat. Genet.* **41**, 199–204 (2009).
4. L. C. Tsoi, S. L. Spain, J. Knight, E. Ellinghaus, P. E. Stuart, F. Capon, J. Ding, Y. Li, T. Tejasvi, J. E. Gudjonsson, H. M. Kang, M. H. Allen, R. McManus, G. Novelli, L. Samuelsson, J. Schalkwijk, M. Ståhle, A. D. Burden, C. H. Smith, M. J. Cork, X. Estivill, A. M. Bowcock, G. G. Krueger, W. Weger, J. Worthington, R. Tazi-Ahnini, F. O. Nestle, A. Hayday, P. Hoffmann, J. Winkelmann, C. Wijmenga, C. Langford, S. Edkins, R. Andrews, H. Blackburn, A. Strange, G. Band, R. D. Pearson, D. Vukcevic, C. C. Spencer, P. Deloukas, U. Mrowietz, S. Schreiber, S. Weidinger, S. Koks, K. Kingo, T. Esko, A. Metspalu, H. W. Lim, J. J. Voorhees, M. Weichenthal, H. E. Wichmann, V. Chandran, C. F. Rosen, P. Rahman, D. D. Gladman, C. E. Griffiths, A. Reis, J. Kere; Collaborative Association Study of Psoriasis (CASP); Genetic Analysis of Psoriasis Consortium; Psoriasis Association Genetics Extension; Wellcome Trust Case Control Consortium 2, R. P. Nair, A. Franke, J. N. Barker, G. R. Abecasis, J. T. Elder, R. C. Trembath, Identification of 15 new psoriasis susceptibility loci highlights the role of innate immunity. *Nat. Genet.* **44**, 1341–1348 (2012).
5. S. K. Mahil, F. Capon, J. N. Barker, Genetics of Psoriasis. *Dermatol. Clin.* **33**, 1–11 (2015).
6. N. Dand, S. Mucha, L. C. Tsoi, S. K. Mahil, P. E. Stuart, A. Arnold, H. Baurecht, A. D. Burden, K. C. Duffin, V. Chandran, C. J. Curtis, S. Das, D. Ellinghaus, E. Ellinghaus, C. Enerback, T. Esko, D. D. Gladman, C. E. M. Griffiths, J. E. Gudjonsson, P. Hoffman, G. Homuth, U. Hüffmeier, G. G. Krueger, M. Laudes, S. H. Lee, W. Lieb, H. W. Lim, S. Löhr, U. Mrowietz, M. Müller-Nurayid, M. Nöthen, A. Peters, P. Rahman, A. Reis, N. J. Reynolds, E. Rodriguez, C. O. Schmidt, S. L. Spain, K. Strauch, T. Tejasvi, J. J. Voorhees, R. B. Warren, M. Weichenthal, S. Weidinger, M. Zawistowski, R. P. Nair, F. Capon, C. H. Smith, R. C. Trembath, G. R. Abecasis, J. T. Elder, A. Franke, M. A. Simpson, J. N. Barker, Exome-wide association study reveals novel psoriasis susceptibility locus at TNFSF15 and rare protective alleles in genes contributing to type I IFN signalling. *Hum. Mol. Genet.* **26**, 4301–4313 (2017).
7. C. T. Jordan, L. Cao, E. D. O. Roberson, K. C. Pierson, C.-F. Yang, C. E. Joyce, C. Ryan, S. Duan, C. A. Helms, Y. Liu, Y. Chen, A. A. McBride, W.-L. Hwu, J.-Y. Wu, Y.-T. Chen, A. Menter, R. Goldbach-Mansky, M. A. Lowes, A. M. Bowcock, PSORS2 is due to mutations in CARD14. *Am. J. Hum. Genet.* **90**, 784–795 (2012).
8. C. T. Jordan, L. Cao, E. D. O. Roberson, S. Duan, C. A. Helms, R. P. Nair, K. C. Duffin, P. E. Stuart, D. Goldgar, G. Hayashi, E. H. Olfson, B.-J. Feng, C. R. Pullinger, J. P. Kane, C. A. Wise, R. Goldbach-Mansky, M. A. Lowes, L. Peddle, V. Chandran, W. Liao, P. Rahman, G. G. Krueger, D. Gladman, J. T. Elder, A. Menter, A. M. Bowcock, Rare and common variants in CARD14, encoding an epidermal regulator of NF-kappaB, in psoriasis. *Am. J. Hum. Genet.* **90**, 796–808 (2012).
9. M. Ammar, C. Bouchlaka-Souissi, C. A. Helms, I. Zaraa, C. T. Jordan, H. Anbunathan, R. Bouhaha, S. Kouidhi, N. Doss, R. Dhaoui, A. B. Osman, A. B. A. El Gaied, R. Marrakchi, M. Mokni, A. M. Bowcock, Genome-wide linkage scan for psoriasis susceptibility loci in multiplex Tunisian families. *Br. J. Dermatol.* **168**, 583–587 (2013).
10. M. Ammar, C. T. Jordan, L. Cao, E. Lim, C. B. Souissi, A. Jrad, I. Omrane, S. Kouidhi, I. Zaraa, H. Anbunathan, M. Mokni, N. Doss, E. Guttman-Yassky, A. B. El Gaaied, A. Menter, A. M. Bowcock, CARD14 alterations in Tunisian patients with psoriasis and further characterization in European cohorts. *Br. J. Dermatol.* **174**, 330–337 (2016).
11. D. Fuchs-Telem, O. Sarig, M. A. M. van Steensel, O. Isakov, S. Israeli, J. Nousbeck, K. Richard, V. Winnepenninckx, M. Vernooij, N. Shomron, J. Uitto, P. Fleckman, G. Richard, E. Sprecher, Familial pityriasis rubra pilaris is caused by mutations in CARD14. *Am. J. Hum. Genet.* **91**, 163–170 (2012).
12. Q. Li, H. J. Chung, N. Ross, M. Keller, J. Andrews, J. Kingman, O. Sarig, D. Fuchs-Telem, E. Sprecher, J. Uitto, Analysis of *CARD14* polymorphisms in pityriasis rubra pilaris: Activation of NF-κB. *J. Invest. Dermatol.* **135**, 1905–1908 (2015).
13. T. Takeichi, K. Sugiura, T. Nomura, T. Sakamoto, Y. Ogawa, N. Oiso, Y. Futei, A. Fujisaki, A. Koizumi, Y. Aoyama, K. Nakajima, Y. Hatano, K. Hayashi, A. Ishida-Yamamoto, S. Fujiwara, S. Sano, K. Iwatsuki, A. Kawada, Y. Suga, H. Shimizu, J. A. McGrath, M. Akiyama, Pityriasis Rubra Pilaris Type V as an autoinflammatory disease by CARD14 mutations. *JAMA Dermatol.* **153**, 66–70 (2017).
14. M. Tanaka, K. Kobiyama, T. Honda, K. Uchio-Yamada, Y. Natsume-Kitatani, K. Mizuguchi, K. Kabashima, K. J. Ishii, Essential role of CARD14 in murine experimental psoriasis. *J. Immunol.* **200**, 71–81 (2018).
15. J. L. Harden, S. M. Lewis, K. C. Pierson, M. Suárez-Fariñas, T. Lentini, F. S. Ortenzio, L. C. Zaba, R. Goldbach-Mansky, A. M. Bowcock, M. A. Lowes, CARD14 expression in dermal endothelial cells in psoriasis. *PLoS ONE* **9**, e111255 (2014).
16. J. Bertin, L. Wang, Y. Guo, M. D. Jacobson, J.-L. Poyet, S. M. Srinivasula, S. Merriam, P. S. DiStefano, E. S. Alnemri, CARD11 and CARD14 are novel caspase recruitment domain (CARD)/Membrane-associated Guanylate Kinase (MAGUK) family members that interact with BCL10 and activate NF-κB. *J. Biol. Chem.* **276**, 11877–11882 (2001).
17. J. Ruland, L. Hartjes, CARD–BCL-10–MALT1 signalling in protective and pathological immunity. *Nat. Rev. Immunol.* **19**, 118–134 (2019).
18. A. Howes, P. A. O'Sullivan, F. Breyer, A. Ghose, L. Cao, D. Krappmann, A. M. Bowcock, S. C. Ley, Psoriasis mutations disrupt CARD14 autoinhibition promoting BCL10-MALT1-dependent NF-κB activation. *Biochem. J.* **473**, 1759–1768 (2016).
19. M. Mellett, B. Meier, D. Mohanan, R. Schairer, P. Cheng, T. K. Satoh, B. Kiefer, C. Ospelt, S. Nobbe, M. Thome, E. Contassot, L. E. French, CARD14 gain-of-function mutation alone is sufficient to drive IL-23/IL-17-mediated psoriasiform skin inflammation in vivo. *J. Invest. Dermatol.* **138**, 2010–2023 (2018).
20. J. P. Sundberg, C. H. Pratt, K. A. Silva, V. E. Kennedy, W. Qin, T. M. Stearns, J. Frost, B. A. Sundberg, A. M. Bowcock, Gain of function p.E138A alteration in Card14 leads to psoriasiform skin inflammation and implicates genetic modifiers in disease severity. *Exp. Mol. Pathol.* **110**, 104286 (2019).
21. M. Wang, S. Zhang, G. Zheng, J. Huang, Z. Songyang, X. Zhao, X. Lin, Gain-of-function mutation of Card14 leads to spontaneous psoriasis-like skin inflammation through enhanced keratinocyte response to IL-17A. *Immunity* **49**, 66–79.e5 (2018).

22. E. Van Nuffel, J. Staal, G. Baudelet, M. Haegman, Y. Driege, T. Hochepied, I. S. Afonina, R. Beyaert, MALT1 targeting suppresses CARD14-induced psoriatic dermatitis in mice. *EMBO Rep.* **21**, e49237 (2020).
23. T. Dainichi, R. Matsumoto, A. Mostafa, K. Kabashima, Immune control by TRAF6-mediated pathways of epithelial cells in the EIME (Epithelial Immune Microenvironment). *Front. Immunol.* **10**, 1107 (2019).
24. L. Wang, Y. Guo, W. J. Huang, X. Ke, J. L. Poyet, G. A. Manji, S. Merriam, M. A. Glucksmann, P. S. DiStefano, E. S. Alnemri, J. Bertin, Card10 is a novel caspase recruitment domain/membrane-associated guanylate kinase family member that interacts with BCL10 and activates NF-κB. *J. Biol. Chem.* **276**, 21405–21409 (2001).
25. I. S. Afonina, E. Van Nuffel, G. Baudelet, Y. Driege, M. Kreike, J. Staal, R. Beyaert, The paracaspase MALT1 mediates CARD14-induced signaling in keratinocytes. *EMBO Rep.* **17**, 914–927 (2016).
26. A. Schmitt, P. Grondona, T. Maier, M. Brändle, C. Schönfeld, G. Jäger, C. Kosnopfel, F. C. Eberle, B. Schittek, K. Schulze-Osthoff, A. S. Yazdi, S. Hailfinger, MALT1 protease activity controls the expression of inflammatory genes in keratinocytes upon zymosan stimulation. *J. Invest. Dermatol.* **136**, 788–797 (2016).
27. M. Rosenbaum, A. Gewies, K. Pechloff, C. Heuser, T. Engleitner, T. Gehring, L. Hartjes, S. Krebs, D. Krappmann, M. Kriegsmann, W. Weichert, R. Rad, C. Kurts, J. Ruland, Bcl10-controlled Malt1 paracaspase activity is key for the immune suppressive function of regulatory T cells. *Nat. Commun.* **10**, 2352 (2019).
28. H. R. Dassule, P. Lewis, M. Bei, R. Maas, A. P. McMahon, Sonic hedgehog regulates growth and morphogenesis of the tooth. *Development* **127**, 4775–4785 (2000).
29. L. van der Fits, S. Mourits, J. S. A. Voerman, M. Kant, L. Boon, J. D. Laman, F. Cornelissen, A.-M. Mus, E. Florencia, E. P. Prens, E. Lubberts, Imiquimod-induced psoriasis-like skin inflammation in mice is mediated via the IL-23/IL-17 Axis. *J. Immunol.* **182**, 5836–5845 (2009).
30. M. Blonska, B. P. Pappu, R. Matsumoto, H. Li, B. Su, D. Wang, X. Lin, The CARMA1-Bcl10 signaling complex selectively regulates JNK2 kinase in the T cell receptor-signaling pathway. *Immunity* **26**, 55–66 (2007).
31. S. A. Watt, K. J. Purdie, N. Y. den Breems, M. Dimon, S. T. Arron, A. T. McHugh, D. J. Xue, J. H. S. Dayal, C. M. Proby, C. A. Harwood, I. M. Leigh, A. P. South, Novel CARD11 mutations in human cutaneous squamous cell carcinoma lead to aberrant NF-κB regulation. *Am. J. Pathol.* **185**, 2354–2363 (2015).
32. K. Sommer, B. Guo, J. L. Pomerantz, A. D. Bandaranayake, M. E. Moreno-García, Y. L. Ovechkina, D. J. Rawlings, Phosphorylation of the CARMA1 linker controls NF-κB activation. *Immunity* **23**, 561–574 (2005).
33. B. S. Baker, L. Brent, H. Valdimarsson, A. V. Powles, L. al-Imara, M. Walker, L. Fry, Is epidermal cell proliferation in psoriatic skin grafts on nude mice driven by T-cell derived cytokines? *Br. J. Dermatol.* **126**, 105–110 (1992).
34. S. P. Singh, H. H. Zhang, J. F. Foley, M. N. Hedrick, J. M. Farber, Human T cells that are able to produce IL-17 express the chemokine receptor CCR6. *J. Immunol.* **180**, 214–221 (2008).
35. Z. Hao, K. Rajewsky, Homeostasis of peripheral B cells in the absence of B cell influx from the bone marrow. *J. Exp. Med.* **194**, 1151–1164 (2001).
36. P. Wong, P. A. Coulombe, Loss of keratin 6 (K6) proteins reveals a function for intermediate filaments during wound repair. *J. Cell Biol.* **163**, 327–337 (2003).
37. R. D. Paladini, K. Takahashi, N. S. Bravo, P. A. Coulombe, Onset of re-epithelialization after skin injury correlates with a reorganization of keratin filaments in wound edge keratinocytes: Defining a potential role for keratin 16. *J. Cell Biol.* **132**, 381–397 (1996).
38. M. A. Lowes, M. Suárez-Fariñas, J. G. Krueger, Immunology of Psoriasis. *Annu. Rev. Immunol.* **32**, 227–255 (2014).
39. J. Ruland, G. S. Duncan, A. Elia, I. del Barco Barrantes, L. Nguyen, S. Plyte, D. G. Millar, D. Bouchard, A. Wakeham, P. S. Ohashi, T. W. Mak, Bcl10 is a positive regulator of antigen receptor–induced activation of NF-κ B and neural tube closure. *Cell* **104**, 33–42 (2001).
40. J. Ruland, G. S. Duncan, A. Wakeham, T. W. Mak, Differential requirement for Malt1 in T and B cell antigen receptor signaling. *Immunity* **19**, 749–758 (2003).
41. L. C. Tsoi, S. L. Spain, E. Ellinghaus, P. E. Stuart, F. Capon, J. Knight, T. Tejasvi, H. M. Kang, M. H. Allen, S. Lambert, S. Stoll, S. Weidinger, J. E. Gudjonsson, S. Koks, K. Kingo, T. Esko, S. Das, A. Metspalu, M. Weichenthal, C. Enerback, G. G. Krueger, J. J. Voorhees, V. Chandran, C. F. Rosen, P. Rahman, D. D. Gladman, A. Reis, R. P. Nair, A. Franke, J. N. Barker, G. R. Abecasis, R. C. Trembath, J. T. Elder, Enhanced meta-analysis and replication studies identify five new psoriasis susceptibility loci. *Nat. Commun.* **6**, 7001 (2015).
42. A. Müller, A. Hennig, S. Lorscheid, P. Grondona, K. Schulze-Osthoff, S. Hailfinger, D. Kramer, IκBζ is a key transcriptional regulator of IL-36–driven psoriasis-related gene expression in keratinocytes. *Proc. Natl. Acad. Sci.* **115**, 10088–10093 (2018).
43. A. Chiricozzi, E. Guttman-Yassky, M. Suárez-Fariñas, K. E. Nograles, S. Tian, I. Cardinale, S. Chimenti, J. G. Krueger, Integrative responses to IL-17 and TNF-α in human keratinocytes account for key inflammatory pathogenic circuits in psoriasis. *J. Invest. Dermatol.* **131**, 677–687 (2011).
44. B. Coornaert, M. Baens, K. Heyninck, T. Bekaert, M. Haegman, J. Staal, L. Sun, Z. J. Chen, P. Marynen, R. Beyaert, T cell antigen receptor stimulation induces MALT1 paracaspase–mediated cleavage of the NF-κB inhibitor A20. *Nat. Immunol.* **9**, 263–271 (2008).
45. L. R. Klei, D. Hu, R. Panek, D. N. Alfano, R. E. Bridwell, K. M. Bailey, K. I. Oravecz-Wilson, V. J. Concel, E. M. Hess, M. Van Beek, P. C. Delekta, S. Gu, S. C. Watkins, A. T. Ting, P. J. Gough, K. P. Foley, J. Bertin, L. M. McAllister-Lucas, P. C. Lucas, MALT1 protease activation triggers acute disruption of endothelial barrier integrity via CYLD cleavage. *Cell Rep.* **17**, 221–232 (2016).
46. L. Israël, M. Bardet, A. Huppertz, N. Mercado, S. Ginster, A. Unterreiner, A. Schlierf, J. F. Goetschy, H.-G. Zerwes, L. Roth, F. Kolbinger, F. Bornancin, A CARD10-dependent tonic signalosome activates MALT1 paracaspase and regulates IL-17/TNF-α–driven keratinocyte inflammation. *J. Invest. Dermatol.* **138**, 2075–2079 (2018).
47. S. Hailfinger, H. Nogai, C. Pelzer, M. Jaworski, K. Cabalzar, J.-E. Charton, M. Guzzardi, C. Décaillet, M. Grau, B. Dörken, P. Lenz, G. Lenz, M. Thome, Malt1-dependent RelB cleavage promotes canonical NF-κB activation in lymphocytes and lymphoma cell lines. *Proc. Natl. Acad. Sci. U.S.A.* **108**, 14596–14601 (2011).
48. T. Uehata, H. Iwasaki, A. Vandenbon, K. Matsushita, E. Hernandez-Cuellar, K. Kuniyoshi, T. Satoh, T. Mino, Y. Suzuki, D. M. Standley, T. Tsujimura, H. Rakugi, Y. Isaka, O. Takeuchi, S. Akira, Malt1-induced cleavage of regnase-1 in CD4+ Helper T cells regulates immune activation. *Cell* **153**, 1036–1049 (2013).
49. H. Tanaka, Y. Arima, D. Kamimura, Y. Tanaka, N. Takahashi, T. Uehata, K. Maeda, T. Satoh, M. Murakami, S. Akira, Phosphorylation-dependent Regnase-1 release from endoplasmic reticulum is critical in IL-17 response. *J. Exp. Med.* **216**, 1431–1449 (2019).
50. A. Gewies, O. Gorka, H. Bergmann, K. Pechloff, F. Petermann, K. M. Jeltsch, M. Rudelius, M. Kriegsmann, W. Weichert, M. Horsch, J. Beckers, W. Wurst, M. Heikenwalder, T. Korn, V. Heissmeyer, J. Ruland, Uncoupling Malt1 threshold function from paracaspase activity results in destructive autoimmune inflammation. *Cell Rep.* **9**, 1292–1305 (2014).
51. F. Schlauderer, K. Lammens, D. Nagel, M. Vincendeau, A. C. Eitelhuber, S. H. L. Verhelst, D. Kling, A. Chrusciel, J. Ruland, D. Krappmann, K.-P. Hopfner, Structural analysis of phenothiazine derivatives as allosteric inhibitors of the MALT1 paracaspase. *Angew. Chem. Int. Ed. Engl.* **52**, 10384–10387 (2013).
52. D. Nagel, S. Spranger, M. Vincendeau, M. Grau, S. Raffegerst, B. Kloo, D. Hlahla, M. Neuenschwander, J. Peter von Kries, K. Hadian, B. Dörken, P. Lenz, G. Lenz, D. J. Schendel, D. Krappmann, Pharmacologic inhibition of MALT1 protease by phenothiazines as a therapeutic approach for the treatment of aggressive ABC-DLBCL. *Cancer Cell* **22**, 825–837 (2012).
53. Y.-J. Zhang, Y.-Z. Sun, X.-H. Gao, R.-Q. Qi, Integrated bioinformatic analysis of differentially expressed genes and signaling pathways in plaque psoriasis. *Mol. Med. Rep.* **20**, 225–235 (2019).
54. T. Oudot, F. Lesueur, M. Guedj, R. de Cid, S. McGinn, S. Heath, M. Foglio, B. Prum, M. Lathrop, J.-F. Prud'homme, J. Fischer, An association study of 22 candidate genes in psoriasis families reveals shared genetic factors with other autoimmune and skin disorders. *J. Invest. Dermatol.* **129**, 2637–2645 (2009).
55. M. Devos, D. A. Mogilenko, S. Fleury, B. Gilbert, C. Becquart, S. Quemener, H. Dehondt, P. Tougaard, B. Staels, C. Bachert, P. Vandenabeele, G. Van Loo, D. Staumont-Salle, W. Declercq, D. Dombrowicz, Keratinocyte expression of A20/TNFAIP3 controls skin inflammation associated with atopic dermatitis and psoriasis. *J. Invest. Dermatol.* **139**, 135–145 (2019).
56. S. K. Ippagunta, R. Gangwar, D. Finkelstein, P. Vogel, S. Pelletier, S. Gingras, V. Redecke, H. Häcker, Keratinocytes contribute intrinsically to psoriasis upon loss of Tnip1 function. *Proc. Natl. Acad. Sci. U.S.A.* **113**, E6162–E6171 (2016).
57. L. Israel, M. Mellett, Clinical and genetic heterogeneity of *CARD14* mutations in psoriatic skin disease. *Front. Immunol.* **9**, 2239 (2018).
58. G. Stelzer, N. Rosen, I. Plaschkes, S. Zimmerman, M. Twik, S. Fishilevich, T. I. Stein, R. Nudel, I. Lieder, Y. Mazor, S. Kaplan, D. Dahary, D. Warshawsky, Y. Guan-Golan, A. Kohn, N. Rappaport, M. Safran, D. Lancet, The GeneCards Suite: From gene data mining to disease genome sequence analyses. *Curr. Protoc. Bioinformatics* **54**, 1.30.1–1.30.33 (2016).
59. P. F. Lizzul, A. Aphale, R. Malaviya, Y. Sun, S. Masud, V. Dombrovskiy, A. B. Gottlieb, Differential expression of phosphorylated NF-κB/RelA in normal and psoriatic epidermis and downregulation of NF-κB in response to treatment with etanercept. *J. Invest. Dermatol.* **124**, 1275–1283 (2005).
60. N. Fyhrquist, G. Muirhead, S. Prast-Nielsen, M. Jeanmougin, P. Olah, T. Skoog, G. Jules-Clement, M. Feld, M. Barrientos-Somarribas, H. Sinkko, E. H. van den Bogaard, P. L. J. M. Zeeuwen, G. Rikken, J. Schalkwijk, H. Niehues, W. Däubener, S. K. Eller, H. Alexander, D. Pennino, S. Suomela, I. Tessas, E. Lybeck, A. M. Baran, H. Darban, R. S. Gangwar, U. Gerstel, K. Jahn, P. Karisola, L. Yan, B. Hansmann, S. Katayama, S. Meller, M. Bylesjö, P. Hupé, F. Levi-Schaffer, D. Greco, A. Ranki, J. M. Schröder, J. Barker, J. Kere, S. Tsoka, A. Lauerma, V. Soumelis, F. O. Nestle, B. Homey, B. Andersson, H. Alenius, Microbe-host interplay in atopic dermatitis and psoriasis. *Nat. Commun.* **10**, 4703 (2019).
61. X. Liu, Q. Cai, H. Yang, Z. Gao, L. Yang, Distribution of *Malassezia* species on the skin of patients with psoriasis. *J. Med. Mycol.* **31**, 101111 (2021).
62. S. M. Rudramurthy, P. Honnavar, A. Chakrabarti, S. Dogra, P. Singh, S. Handa, Association of Malassezia species with psoriatic lesions. *Mycoses* **57**, 483–488 (2014).

63. Y. Sasaki, E. Derudder, E. Hobeika, R. Pelanda, M. Reth, K. Rajewsky, M. Schmidt-Supprian, Canonical NF-κB Activity, Dispensable for B Cell development, replaces BAFF-receptor signals and promotes B cell proliferation upon activation. *Immunity* **24**, 729–739 (2006).
64. K. Pechloff, J. Holch, U. Ferch, M. Schweneker, K. Brunner, M. Kremer, T. Sparwasser, L. Quintanilla-Martinez, U. Zimber-Strobl, B. Streubel, A. Gewies, C. Peschel, J. Ruland, The fusion kinase ITK-SYK mimics a T cell receptor signal and drives oncogenesis in conditional mouse models of peripheral T cell lymphoma. *J. Exp. Med.* **207**, 1031–1044 (2010).
65. C. Malosse, S. Henri, Isolation of mouse dendritic cell subsets and macrophages from the skin. *Methods Mol. Biol.* **1423**, 129–137 (2016).
66. L. Li, Mouse epidermal keratinocyte culture. *Methods Mol. Biol.* **945**, 177–191 (2013).
67. D. Kim, B. Langmead, S. L. Salzberg, HISAT: A fast spliced aligner with low memory requirements. *Nat. Methods* **12**, 357–360 (2015).
68. M. Pertea, G. M. Pertea, C. M. Antonescu, T.-C. Chang, J. T. Mendell, S. L. Salzberg, StringTie enables improved reconstruction of a transcriptome from RNA-seq reads. *Nat. Biotechnol.* **33**, 290–295 (2015).
69. M. I. Love, W. Huber, S. Anders, Moderated estimation of fold change and dispersion for RNA-seq data with DESeq2. *Genome Biol.* **15**, 550 (2014).
70. D. W. Huang, B. T. Sherman, R. A. Lempicki, Systematic and integrative analysis of large gene lists using DAVID bioinformatics resources. *Nat. Protoc.* **4**, 44–57 (2009).
71. D. W. Huang, B. T. Sherman, R. A. Lempicki, Bioinformatics enrichment tools: Paths toward the comprehensive functional analysis of large gene lists. *Nucleic Acids Res.* **37**, 1–13 (2009).
72. A. Subramanian, P. Tamayo, V. K. Mootha, S. Mukherjee, B. L. Ebert, M. A. Gillette, A. Paulovich, S. L. Pomeroy, T. R. Golub, E. S. Lander, J. P. Mesirov, Gene set enrichment analysis: A knowledge-based approach for interpreting genome-wide expression profiles. *Proc. Natl. Acad. Sci. U.S.A.* **102**, 15545–15550 (2005).
73. V. K. Mootha, C. M. Lindgren, K.-F. Eriksson, A. Subramanian, S. Sihag, J. Lehar, P. Puigserver, E. Carlsson, M. Ridderstråle, E. Laurila, N. Houstis, M. J. Daly, N. Patterson, J. P. Mesirov, T. R. Golub, P. Tamayo, B. Spiegelman, E. S. Lander, J. N. Hirschhorn, D. Altshuler, L. C. Groop, PGC-1α-responsive genes involved in oxidative phosphorylation are coordinately downregulated in human diabetes. *Nat. Genet.* **34**, 267–273 (2003).

Acknowledgments: We would like to thank V. Höfl, T. Neumayer, K. Burmeister, N. Prause, O. Seelbach, R. Secci, M. Utzt, S. Engels, and K. Drobe for outstanding technical assistance; R. Öllinger and R. Rad for assistance in RNA sequencing; and P.-A. König and K. Li for excellent discussions and comments. **Funding:** This work was supported by the German Research Foundation (Project-ID 210592381 – SFB 1054 to J.R. and T.K.; Project-ID 360372040 – SFB 1335 to J.R., K.S., and T.B.; Project-ID 395357507 – SFB 1371 to J.R., K.S., and T.B.; and Project-ID 369799452 – TRR 237, RU 695/9-1 to J.R.); by the European Research Council (ERC) under the European Union's Horizon 2020 research and innovation programme (grant agreement no. 834154) (to J.R.); by the German Research Foundation (SFB TR 128 to T.K.); by the German Research Foundation (Synergy) (to T.K.); by the German Ministry for Education and Research (KKNMS, T-B in NMO) (to T.K.); by the European Research Council (CoG 647215) (to T.K.); and by the German Research Foundation (SFB 824 B10 to T.B. and BI696/10-1 to T.B.). L.V.K. is a recipient of the János Bolyai Research Scholarship of the Hungarian Academy of Sciences.
Author contributions: Conceptualization: Z.K. and J.R. Investigation: Z.K., L.V., K.P., L.V.K., T.W., A.M., A.J., K.K., L.H., E.H., S.M., K.S., and T.B. Providing materials: M.M., L.E.F., and T.V. Funding acquisition: T.B., T.K., and J.R. Writing (original draft): Z.K. and J.R. Writing (review and editing): All authors. **Competing interests:** The authors declare that they have no competing interests. T.B. gave advice to or got honorarium for talks or research grant from the following companies: Abbvie, Alk-Abelló, Celgene-BMS, Galderma, GlaxoSmithKline, Leo Pharma, Lilly Deutschland GmbH, Mylan, Novartis, Phadia-Thermo Fisher, Sanofi-Genzyme, Regeneron, and Viatris. K.S. is consultant for Roche Pharma AG and is advisory board member of TRIMT. However, none of these additional affiliations will benefit from this research. **Data and materials availability:** The RNA-seq datasets generated during this study are deposited in NCBI's Gene Expression Omnibus under the association numbers GSE185998 and GSE185999. All other data needed to evaluate the conclusions in the paper are present in the paper or the Supplementary Materials. Proprietary transgenic mice are available from the corresponding author with a material transfer agreement upon reasonable request.

Submitted 10 March 2021
Accepted 20 October 2021
Published 26 November 2021
10.1126/sciimmunol.abi4425